

SUMMARY

Aerodynamics: Typical Questions
MECA-Y402

Author:
Mischa MASSON

Professors:
Herman DECONINCK
Chris LACOR

Year 2016 - 2017

Appel à contribution

Synthèse Open Source



Ce document est grandement inspiré de l'excellent cours donné par Herman DECONINCK et Chris LACOR à l'EPB (École Polytechnique de Bruxelles), faculté de l'ULB (Université Libre de Bruxelles). Il est écrit par les auteurs susnommés avec l'aide de tous les autres étudiants et votre aide est la bienvenue ! En effet,

il y a toujours moyen de l'améliorer surtout que si le cours change, la synthèse doit être changée en conséquence. On peut retrouver le code source à l'adresse suivante

<https://github.com/nenglebert/Syntheses>

Pour contribuer à cette synthèse, il vous suffira de créer un compte sur *Github.com*. De légères modifications (petites coquilles, orthographe, ...) peuvent directement être faites sur le site ! Vous avez vu une petite faute ? Si oui, la corriger de cette façon ne prendra que quelques secondes, une bonne raison de le faire !

Pour de plus longues modifications, il est intéressant de disposer des fichiers : il vous faudra pour cela installer *LATEX*, mais aussi *git*. Si cela pose problème, nous sommes évidemment ouverts à des contributeurs envoyant leur changement par mail ou n'importe quel autre moyen.

Le lien donné ci-dessus contient aussi un README contenant de plus amples informations, vous êtes invités à le lire si vous voulez faire avancer ce projet !

Licence Creative Commons

Le contenu de ce document est sous la licence Creative Commons : *Attribution-NonCommercial-ShareAlike 4.0 International (CC BY-NC-SA 4.0)*. Celle-ci vous autorise à l'exploiter pleinement, compte-tenu de trois choses :



1. *Attribution* ; si vous utilisez/modifiez ce document vous devez signaler le(s) nom(s) de(s) auteur(s).
2. *Non Commercial* ; interdiction de tirer un profit commercial de l'œuvre sans autorisation de l'auteur
3. *Share alike* ; partage de l'œuvre, avec obligation de rediffuser selon la même licence ou une licence similaire

Si vous voulez en savoir plus sur cette licence :

<http://creativecommons.org/licenses/by-nc-sa/4.0/>

Merci !

Contents

1 Explain how lift can generated around an airfoil for inviscid incompressible flow.	3
1.1 Explain the origin of the bound vortex which exists around a profile which generates lift. Explain using the Kelvin theorem	3
1.2 What is the start-up vortex, what happens with it when the flow reaches a steady state	3
1.3 Explain the Kutta condition	4
2 Derive an expression for the aerodynamic lift of on airfoil for inviscid incompressible flow (i.e. neglecting viscous effects).	4
2.1 Express conservation of momentum over a closed surface S far away from the wing, neglecting viscous forces	5
2.2 Show that the lift force is linked to the vorticity through the closed surface S . .	6
2.3 Show that for the 2D airfoil the lift force is linked to the circulation around the airfoil, derive the Kutta-Joukowski formula for the lift generated by a 2D profile	6
3 Characteristics of a 2D airfoil:	6
3.1 Define lift and drag, give the principle components of lift and drag force in normal operation and in case of separation	6
3.2 Explain the non-dimensional force coefficients(C_l , C_d , C_m) and which are the similarity parameters influencing these coefficients	7
3.3 Explain:	8
3.4 Compute the Location of the center of pressure CP as a function of the angle of attack alpha	8
3.5 Explain the lift, drag and moment curves as a function of the angle of attack alpha	9
3.6 Explain what is stall and critical angle of attack. Explain different types of stall.	9
3.7 Discuss the polar curve of the airfoil, i.e. lift coefficient as a function of drag coefficient, show the glide ratio on this plot	10
3.8 What is the importance of the glide ratio, discuss the case of a gliding plane (engine off situation)	10
4 Computation of inviscid irrotational flow around a 2D airfoil using conformal mapping - Joukowski profiles	11
4.1 Explain methods based on complex potential function, explain the connection with usual stream function and potential function	11
4.2 Explain how the velocity can be computed from the complex potential function .	12
4.3 Derive the complex potential function for uniform flow, source/sink flow, free vortex	12
4.3.1 Uniform flow	12
4.3.2 Source / Sink	12
4.3.3 Free vortex	13
4.4 Compute flow around Rankine body and around a cylinder	13
4.5 Explain how a the class of Joukowski profiles is obtained by conformal mapping of a circle	14
5 Computation of inviscid irrotational flow around a thin airfoil based on a continuous distribution of vortices	15
5.1 Explain what is a free vortex	15

5.2	Explain what is a continuous distribution of free vortices on a line	15
5.3	Explain principle of the method of free vortex distribution applied thin airfoils, limitations and hypotheses	15
5.4	Establish the integral equation which allows to compute the vortex distribution for a given profile	16
5.5	Show how to solve this equation using a spectral method, i.e. by expressing the vortex distribution as a truncated Fourier series	17
5.6	How is the Kutta-Youkowsky condition imposed (allowing to compute the lift) . .	18
5.7	Starting from the expressions for the Fourier coefficients, compute the circulation and lift coefficient as a function of angle of attack, explain the result	18
5.7.1	Calculation of the total circulation	18
5.7.2	Calculation of the lift coefficient	18
5.8	Starting from the expression for the momentum coefficient at the leading edge $c_m(\text{LE})$, show that it's a linear function of the lift coefficient c_l	19
5.9	Compute the location of the aerodynamic center AC and the momentum coefficient in the aerodynamic center	19
5.10	Compute the location of the center of pressure	19
6	Computation of inviscid irrotational flow around a thin airfoil based on a continuous distribution of vortices	20
7	3D wing theory	21
7.1	Explain mean chord, span, aspect ratio, taper, sweep of wing	21
7.2	Explain downwash effect, downwash angle, effective angle of attack, total and induced drag	21
7.3	Starting from the given expression for the downwash angle, compute the induced drag force and the induced drag coefficient	22
7.4	Explain the lift curve as a function of the angle of attack for a 3D wing, compare with the lift curve for a 2D profile	22
7.5	Give the expression for the total drag coefficient as a function of C_L	22
7.6	Give the expression of the drag force D as a function of the velocity at infinity .	23
8	3D wing theory – Derivation of Prandtl lifting line method Give the basic ideas and the development of Prandtl's lifting line theory	23
8.1	Velocity induced by a vortex filament	23
8.2	Helmholtz theorems, Biot-Savart law	24
8.3	Circulation around a vortex sheet	24
8.4	Downwash velocity induced by a single horseshoe vortex, why this model for a wing is not working	24
8.5	Downwash velocity induced by a superposition of horseshoe vortices	25
8.6	Derivation of Prandtl's fundamental equation of lifting line theory	25
9	3D wing theory: application of Prandtl lifting line theory for a wing with given circulation Starting from Prandtl's fundamental equation of lifting line theory and the formula for the induced angle of attack:	26
9.1	Discuss the different terms of the equation	26
9.2	Apply to a wing with a given circulation distribution: find lift and drag coefficients	26
9.3	Apply to a wing with a given shape and unknown circulation distribution defined by a truncated Fourier series and compute the lift C_L and the induced drag C_{Di} coefficients	26

9.4	Apply to a tapered wing	27
9.5	Assume an elliptic distribution for the circulation. Show that the platform of the wing must be an ellipse.	28
10	2D airfoil in compressible flow	29
10.1	Derive the compressible potential equation	29
10.2	Assume a thin airfoil at small angle of attack: derive the linearized potential equation. What is the range of validity as a function of the free stream Mach number	29
10.3	Discuss the type of this equation as a function of free stream Mach number, what are the consequences	29
11	2D airfoil compressible flow around an airfoil using the small perturbation approach	29
11.1	Derive the equation governing compressible potential equation, what are the assumptions	29
11.2	Derive the equation in the case of small perturbations. What are the assumptions for this equation to be valid ?	30
11.3	Discuss the application to an airfoil in supersonic flow: lift coefficient, influence of the Mach number, Ackeret formula, lift and drag formula	33
11.3.1	Application to a flat plate	34
11.4	What is wave drag ? discuss supersonic flow over double wedge profile	34
11.5	Transonic flow over a profile: what is critical free stream Mach number(+ discussion), what is drag divergence Mach number	36
11.5.1	Critical Mach number	36
11.5.2	Drag divergence Mach number	37
11.6	Compute the lift coefficient for a 2D profile in compressible flow, assuming that the lift coefficient for the same airfoil is known for incompressible flow.	39
11.7	Discuss the graph giving the slope of the lift curve as a function of the free stream Mach number ($M_{infinity}$)	39
12	Discuss effect of sweep on performance of a 3D wing in compressible flow – Influence on Lift and drag	39
12.1	Lift of swept wings	40
12.2	Lift coefficient as a function of the angle of attack for swept wings	40
12.3	Influence of the sweep angle on the drag	40
13	title	41
13.1	title	41
13.2	title	41
13.3	title	41

1 Explain how lift can be generated around an airfoil for inviscid incompressible flow.

See

Q2

for

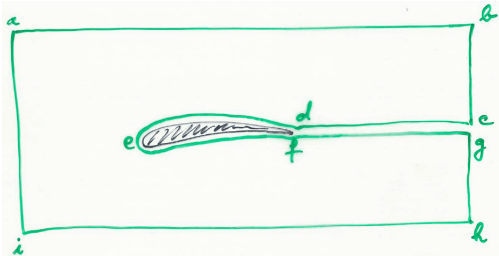


Figure 1

mathematical

explanation.

When looking at an airfoil, we have a pressure that is applied around it. This pressure is non uniform, due to the presence of the airfoil. The integral of pressures over the surface gives a force expressed as the product of the incoming speed and the vorticity vector: the lift.

1.1 Explain the origin of the bound vortex which exists around a profile which generates lift. Explain using the Kelvin theorem

In inviscid case, the Kelvin theorem states that there cannot be vorticity, so no lift. If we take an arbitrary contour around the airfoil we will have no circulation. In inviscid case we can never get a lift \rightarrow D'Alembert paradox. At the trailing edge, if the flow wants to continue on the other corner from below, the velocity must be infinity so that the flow separates. But this is not the case in reality.

To satisfy the Kutta condition (the flow has to leave the airfoil smoothly), there needs to be circulation if we take a contour that contains the airfoil, but for all contour that does not contain the airfoil it is null. Γ varies with the stagnation point position, but only one corresponds to the Kutta condition.

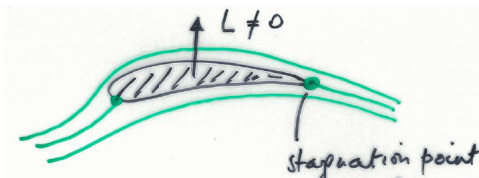


Figure 2

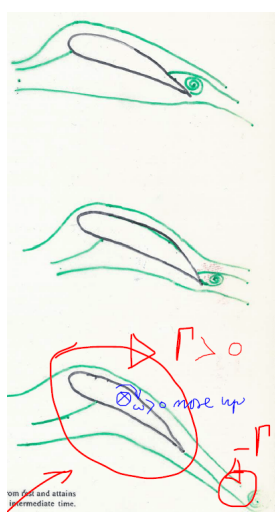


Figure 3

The bound vortex is the vortex around the airfoil. It is compensated by a starting vortex that detaches from the airfoil.

We can show that every contour containing the airfoil has a non 0 circulation. Let's proof that a contour that doesn't contain the airfoil has $\Gamma = 0$:

$$\oint_C \vec{v} d\vec{l} = \oint_{\text{airfoil}} \vec{v} d\vec{l} + \oint_{cd} \vec{v} d\vec{l} + \oint_{fg} \vec{v} d\vec{l} = 0. \quad (1)$$

As the contour elements are exactly opposed to each other, the result is null.

1.2 What is the start-up vortex, what happens with it when the flow reaches a steady state

What happens is that initially we have the first kind of flow, then the formation of the starting vortex due to viscous effects (separation) which is compensated by a **bound vortex** around the airfoil (to respect Kelvin theorem of irrotational flow) that makes $\Gamma \neq 0$. Then the vortex goes away to infinity. Indeed if we take $R = \rho v_\infty \Gamma$, $\Gamma \neq 0$, so we have lift.

1.3 Explain the Kutta condition

The Kutta condition states that the flow can only have a stagnation point at the trailing edge. If this was not the case, the underwing flow would need to accelerate "going backwards" to meet the upperwing flow, see figure 2.

2 Derive an expression for the aerodynamic lift of an airfoil for inviscid incompressible flow (i.e. neglecting viscous effects).

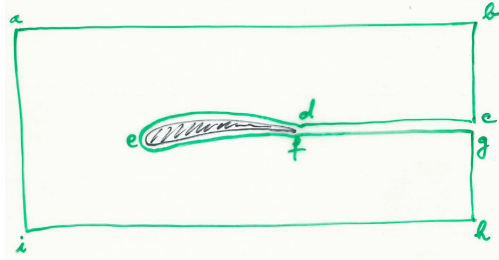


Figure 4

The fundamental integral form of the mass conservation equation is:

$$\frac{d}{dt} \int_V \rho dV + \oint_S \rho \vec{v} d\vec{S} = 0. \quad (2)$$

By applying Gauss theorem $\oint_S \vec{a} \cdot \vec{n} dS = \int_V \nabla \cdot \vec{a} dV$:

$$\int_V \left[\frac{d\rho}{dt} + \nabla \cdot (\rho \vec{v}) \right] dV = 0. \quad (3)$$

True for all volumes:

Continuity equation

$$\frac{d\rho}{dt} + \nabla \cdot (\rho \vec{u}) = 0 \quad (4)$$

General form of the momentum equation is:

$$\rho \ddot{\vec{v}} = \frac{\partial \rho \vec{v}}{\partial t} + \rho (\vec{v} \nabla) \vec{v} = -\nabla p + \nabla \bar{\tau}. \quad (5)$$

Steady state, time derivative goes away. If we consider the x component of the velocity, we can expand the derivative to the whole left term as:

$$\rho (\vec{v} \nabla) v_x = \nabla (\rho \vec{v} v_x) - v_x \nabla (\rho \vec{v}) \quad (6)$$

where the last term is null related to (4) in steady state. Integrating both sides around the volume contained in the closed surface S (abcdefghi on figure) in (6), and applying Gauss theorem, we obtain:

$$\oint_S \vec{v} (\rho \vec{v} \vec{n}) dS = - \oint_S p d\vec{S} + \oint_S \bar{\tau} d\vec{S}. \quad (7)$$

New closed contour $S^* = S - \text{airfoil} - cd - fg$ (previous abhi in fact). (7) becomes:

$$\begin{aligned} & \oint_{S^*} \vec{v} (\rho \vec{v} d\vec{S}) + \oint_{\text{airfoil}} \vec{v} (\rho \vec{v} d\vec{S}) + \oint_{cd+fg} \vec{v} (\rho \vec{v} d\vec{S}) \\ &= - \oint_{S^*} p d\vec{S} - \oint_{\text{airfoil}} p d\vec{S} - \oint_{ed+fg} p d\vec{S} + \oint_{S^*} \bar{\tau} d\vec{S} + \oint_{\text{airfoil}} \bar{\tau} d\vec{S} + \oint_{ed+fg} \bar{\tau} d\vec{S} \end{aligned} \quad (8)$$

Forces applied to a wing:

$$\vec{R} = \oint_{\text{airfoil}} p d\vec{S} - \oint_{\text{airfoil}} \bar{\tau} d\vec{S} \quad (9)$$

$$\oint_{S^*} \vec{v}(\rho \vec{v} d\vec{S}) = - \oint_{S^*} p d\vec{S} + \oint_{S^*} \vec{\tau} d\vec{S} - \vec{R}. \quad (10)$$

Pressure effects induced by the body remains at a long distance from the body. We have to analyse the **non uniform** p along S^* . In order to apply Bernoulli equation $p + \frac{1}{2}\rho v^2 = cst$, let's add the constants p_∞ and v_∞ to (10), as $\oint p_\infty d\vec{S} = p_\infty \oint d\vec{s} = 0$:

$$\vec{R} = - \oint_{S^*} (p - p_\infty) d\vec{S} - \oint_{S^*} (\vec{v} - \vec{v}_\infty) d\vec{m} \quad (11)$$

Let's express $\vec{v} = \vec{v}_\infty + \vec{\delta}_c$ with $\vec{\delta}_c$ a perturbation. Introducing this in Bernoulli equation:

$$p_\infty + \frac{1}{2}\rho \vec{v}_\infty^2 = p + \frac{1}{2}\rho(\vec{v}_\infty + \vec{\delta}_c)^2 = p + \frac{1}{2}\rho(\vec{v}_\infty^2 + 2\vec{v}_\infty \vec{\delta}_c + \vec{\delta}_c^2) \Rightarrow p - p_\infty = -\rho \vec{v}_\infty \vec{\delta}_c. \quad (12)$$

If we replace this result in (11), we find:

$$\vec{R} = \oint_{S^*} \rho[(\vec{v}_\infty \vec{\delta}_c) d\vec{S} - \vec{\delta}_c[(\vec{v}_\infty \cdot d\vec{S})]] \quad (13)$$

by using a vector property $\vec{a} \times (\vec{b} \times \vec{c}) = (\vec{a} \vec{b})\vec{c} - (\vec{a} \vec{c})\vec{b}$:

$$= \rho \vec{v}_\infty \times \oint_{S^*} \vec{\delta}_c \times d\vec{S} = \rho \vec{v}_\infty \times \left[\oint_{S^*} \vec{v} \times d\vec{S} - \oint_{S^*} \vec{v}_\infty \times d\vec{S} \right] \quad (14)$$

and by applying Stokes theorem $\oint_S \vec{a} \times d\vec{S} = \int_V \nabla \times \vec{a} dV$:

$$= \rho \vec{v}_\infty \times \int (\nabla \times \vec{v}) dV = \rho \vec{v}_\infty \times \int \vec{\omega} dV \quad (15)$$

where $\vec{\omega}$ is the **vorticity vector** of direction $\vec{1}_z$ (pointing in the paper):

$$\vec{\omega} = \begin{vmatrix} \vec{1}_x & \vec{1}_y & \vec{1}_z \\ \partial_x & \partial_y & 0 \\ v_x & v_y & 0 \end{vmatrix} = [\partial_x v_y - \partial_y v_x] \vec{1}_z \quad (16)$$

This shows that the lift force is always perpendicular to the flow!

2.1 Express conservation of momentum over a closed surface S far away from the wing, neglecting viscous forces

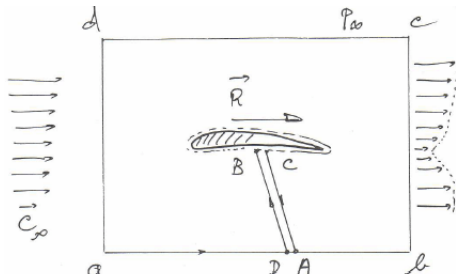


Figure 5

horizontal so that $\vec{R} = R \vec{1}_x$, at the inlet we have \vec{v} and \vec{n} are opposed while at the outlet they are in the same direction:

By considering this (assumption of far field), we can compute the force only by knowing the far field parameters. Indeed, uniform pressure implies null surface integral, so that (10) becomes:

$$\vec{R} = - \oint_{S^*} \vec{v}(\rho \vec{v} d\vec{S}). \quad (17)$$

The velocity term remains, as by experience we know that there is a **wake** making the velocity profile non-uniform. Let's now consider that the velocity is horizontal so that $\vec{R} = R \vec{1}_x$, at the inlet we have \vec{v} and \vec{n} are opposed while at the outlet they are in the same direction:

$$\vec{R} = \int_a^d \vec{v} d\dot{m} - \int_b^e \vec{v} d\dot{m} > 0 \quad (18)$$

showing that there is only **drag** force.

2.2 Show that the lift force is linked to the vorticity through the closed surface S

See above.

2.3 Show that for the 2D airfoil the lift force is linked to the circulation around the airfoil, derive the Kutta-Joukowski formula for the lift generated by a 2D profile

We will now introduce the circulation $\Gamma = -\oint \vec{v} d\vec{l} > 0$ around a body. The convention is to take the anticlockwise direction for $d\vec{l}$ and so for Γ to be > 0 we must have \vec{v} in the clockwise direction. There is a link between the lift force and the circulation. Let's introduce **Stokes theorem**:

$$\oint \vec{a} d\vec{l} = \int_S (\nabla \times \vec{a}) d\vec{S} \quad \Rightarrow -\Gamma = \int_S \vec{\omega} d\vec{S}. \quad (19)$$

We remember that:

$$\begin{aligned} \vec{R} &= \rho \vec{v}_\infty \times \int \vec{\omega} dV = \rho \vec{v}_\infty \times \int l \vec{\omega} dS \quad \Leftrightarrow \frac{\vec{R}}{l} = \rho \vec{v}_\infty \times \int \vec{\omega} dS \\ \frac{\vec{R}}{l} &= \rho \vec{v}_\infty \times \int \vec{\omega} (d\vec{S} \cdot \vec{l}_z) = \rho \vec{v}_\infty \times (-\Gamma) \vec{l}_z = \rho v_\infty \Gamma \vec{l}_y \end{aligned} \quad (20)$$

to finally obtain a very good approximation of the lift:

Kutta formula for lift 2D airfoil

$$|R| = \rho v_\infty \Gamma \quad (21)$$

3 Characteristics of a 2D airfoil:

3.1 Define lift and drag, give the principle components of lift and drag force in normal operation and in case of separation

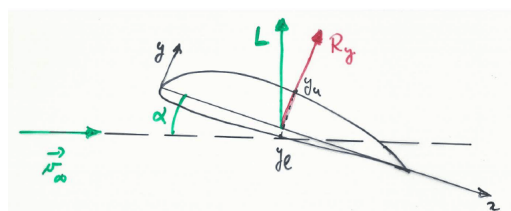


Figure 6

Force applied on the wing:

$$\vec{R} = -\oint p d\vec{S} + \oint \bar{\tau} d\vec{S} \quad (22)$$

with an external normal to the airfoil. The angle of attack is represented on Figure 6.

The pressure term is responsible for lift and the friction term is responsible for drag. Friction forces work tangential to the airfoil and the pressure forces are perpendicular, if there is **no separation** in the flow. The drag created by the stress is called the **skin or friction** drag. Note that in a subsonic inviscid incompressible flow, we have the paradox of d'Alembert because we

have no drag. This shows that the pressure only contributes to lift.

Separation: region above the airfoil where $p - p_\infty \approx 0 \Rightarrow$ high pressure below $p \gg p_\infty$ that slows down the wing. This implies that the applied force is higher than the case without separation and due to the attack angle, the drag force too. This phenomenon is called **pressure drag** (form drag), and here the pressure contributes to drag.

3.2 Explain the non-dimensional force coefficients (C_l , C_d , C_m) and which are the similarity parameters influencing these coefficients

Let's look to the non-dimensional parameters that will influence the lift, the drag and the momentum. We have to define some reference quantities:

$$\begin{aligned} L_{ref} &= C & v_{ref} &= v_\infty & t_{ref} &= L_{ref}/v_{ref} & \rho_{ref} &= \rho_\infty \\ t' &= t/t_{ref} & p_{ref} &= \rho_{ref} \frac{v_{ref}^2}{2} & \text{Mach} &= V_{ref}/a_{ref} & a_{ref} &= \gamma\pi T_{ref} \\ \gamma &= c_p/c_v & Re_{ref} &= \frac{\rho_{ref} v_{ref} L_{ref}}{\mu_{ref}} \end{aligned} \quad (23)$$

where a is the speed of sound. By replacing all these in the mass, momentum and energy equations, we obtain the non-dimensional ones (see Fluid Mechanics II):

$$\begin{aligned} &\bullet \frac{\partial \rho'}{\partial t'} + \nabla(\rho' \vec{v}') = 0 \\ &\bullet \rho' \frac{d\vec{v}'}{dt'} = -\frac{1}{\gamma M_{ref}^2} \nabla p' + \frac{1}{Re_{ref}} \nabla \bar{\tau}' \\ &\bullet \frac{d}{dt'}(\rho' e') + \frac{\gamma(\gamma-1)}{2} M_{ref}^2 \frac{d}{dt'}(\rho' \vec{v}'^2) \\ &= \frac{\gamma}{Pr_{ref} Re_{ref}} \nabla(k' \nabla T') - (\gamma-1) \nabla(p' \vec{v}') + \gamma(\gamma-1) \frac{M_{ref}^2}{Re_{ref}} \nabla(\bar{\tau}' \vec{v}') \end{aligned} \quad (24)$$

We can see that a solution can only be function of 4 parameters: $M, Re, Pr = \frac{c_p \mu}{k}, \gamma$, but we know that the geometry and the angle of attack α have a role by means of the boundary conditions. Then, we assume that the fluid is air ($\gamma = 1.4$) and that we can neglect heat effects (no influence of Pr , incompressible and so low speed flows). The non-dimensional lift, drag and moment are thus function of M, Re , geometry and α . We can define **lift**, **drag** and **moment coefficient** as (we forget about compressibility $\rightarrow M$, and Re effects are low for C_L and C_M):

$$\begin{aligned} C_L(M, Re, geometry, \alpha) &= \frac{L}{\frac{1}{2} \rho_{ref} v_{ref}^2 S} \\ C_D(M, Re, geometry, \alpha) &= \frac{D}{\frac{1}{2} \rho_{ref} v_{ref}^2 S} \\ C_M(M, Re, geometry, \alpha) &= \frac{M}{\frac{1}{2} \rho_{ref} v_{ref}^2 Sc} \end{aligned} \quad (25)$$

where L, D, M are the **dimensional** forces, c the mean chord (S/b) and S a reference surface (3D wing \rightarrow total wing surface, 2D wing $\rightarrow S = c$). We can experimentally show that the lift increases mainly linearly with α and the drag force is caused by friction effects and pressure differences involving with α . This gives the following equations (lower case for 2D):

$$c_l = m(\alpha - \alpha_{L_0}) \quad c_d = c_{d_0} + k c_l^2 \quad (26)$$

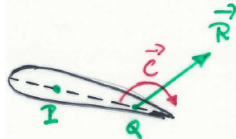
where $m \approx 2\pi$ theoretically and 5.7 practically, k is a constant of order of magnitude 0.01.

3.3 Explain:

center of pressure CP: It's the x value on the chord where the carrier of the force \vec{R} intersects the chord. It's function of the angle of attack. Indeed, if alpha increases, the suction peak will be higher, this induces that the center of pressure move forward (participation of the forward pressure more important).

Note that the center of pressure is not a fixed point. Indeed, it varies with the angle of attack: if $\alpha \nearrow$, the pressure peak on the LE is more important making the x_p move upstream, and the contrary for $\alpha \searrow$. This notion will be completed by the **zero lift angle** α_0 .

equivalent force system in an arbitrary point Q on the chord of the profile:



The force at the pressure center P is equivalent to another force in point Q, but by adding the moment to compensate the one added by moving the force. This moment is:

$$\vec{C}_Q = -\vec{PQ} \times \vec{R}. \quad (27)$$

Figure 7

aerodynamic center AC: Suppose that there is a point Q where the couple C_Q is independent of the angle of attack (because the pressure center changes with alpha). This point is called the aerodynamic center.

The moment at this point is always nose-down and the point is situated upstream to the center of pressure.

the graph of the momentum coefficient c_m at a point Q versus the lift coefficient c_l for Q located at the trailing edge, at the leading edge and at the aerodynamic center of the profile: It is shown experimentally that:

$$c_m(Q) = c_{m0} + k c_l \quad (28)$$

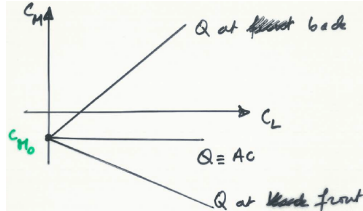


Figure 8

k is a constant that is related to the reference point chosen. If Q is taken on the LE for example, increasing α will produce an increase of the lift and make the center of pressure move upstream. The L increase will compensate the moving x_p such that the moment becomes even more nose-down (more negative following \vec{l}_z) $\Rightarrow k < 0$ for a decrease in (28). The same reasoning applied on the trailing edge gives $k > 0$.

3.4 Compute the Location of the center of pressure CP as a function of the angle of attack alpha

$$\begin{aligned} 1) \quad c_m &= c_{m0} + k c_l & 2) \quad M_{ac} &= (x_{ac} - x_{cp}) N \\ 3) \quad m_{ac} &= M_{AC} = M_0 < 0 & 4) \quad N &= n(\alpha - \alpha_0) \end{aligned} \quad (29)$$

The AC being always upstream the CP the difference in 2) is < 0 . In 4), $n > 0$. By using equation 3,4 and 2, we can compute:

$$M_0 = -(x_{cp} - x_{ac}).n(\alpha - \alpha_0) \Leftrightarrow -\frac{M_0}{n} = (x_{cp} - x_{ac}).(\alpha - \alpha_0) \quad (30)$$

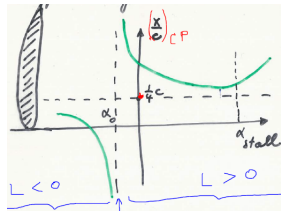


Figure 9

This is the equation of an **hyperbola**. To see it, we only have to compute the limits:

$$\begin{aligned} x_{cp} &= x_{ac} - \frac{M_0}{n} \frac{1}{\alpha - \alpha_0} \\ \lim_{\alpha \rightarrow \pm\infty} x_{cp} &= x_{ac} \quad \lim_{\alpha \rightarrow \alpha_0 > 0} x_{cp} = +\infty \quad \lim_{\alpha \rightarrow \alpha_0 < 0} x_{cp} = -\infty \end{aligned} \quad (31)$$

Let's finally say that commonly, $x_{ac} = cst \approx \frac{1}{4}C$.

3.5 Explain the lift, drag and moment curves as a function of the angle of attack alpha

Starting from what is said in 3.2, experiment showed that lift is increasing linearly with α , and drag goes proportionnaly to c_l^2 . The moment is proportionnal to c_l , we thus expect it to be linear with respect to α .

3.6 Explain what is stall and critical angle of attack. Explain different types of stall.

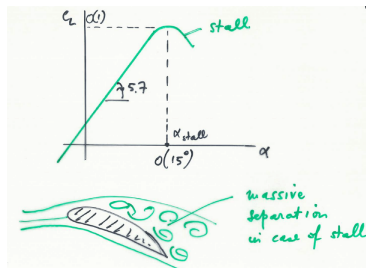


Figure 10

At a certain angle of attack ($\approx 15^\circ$), the lift suddenly drops. This is due to massive separation on the suction side (reverse pressure gradient too high) and happens at the **critical angle of attack**. This phenomenon is called **stall**. In the separated part, the pressure will no longer decrease and will form a pressure plateau.

We have to make the difference between leading-edge stall and trailing-edge stall. For **leading-edge stall**, the massive separation occurs suddenly near the LE resulting

in a strong and sudden drop of lift, when at maximum lift. This especially occurs to thin airfoils with cross-sections between 10 and 16% of the chord. For the **trailing-edge stall**, the point of separation gradually goes upstream with increasing angle of attack resulting in a more gradual drop of lift (more thick airfoils). The comparison is done on the right figure. We can also see a third type of stall called **thin airfoil stall** with the example of a flat plate.

In conclusion, the LE must be sufficiently rounded to have a good maximum lift. In fact the profile may nor be too

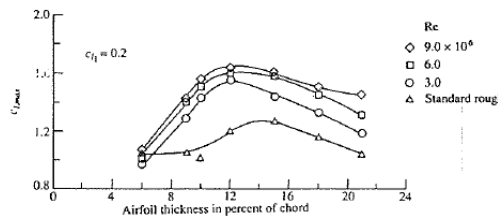


Figure 12

Notice that the camber have also an effect on maximum lift, the best is a camber of 8 up to 10%.

$$L = C_L \frac{1}{2} \rho_{ref} v_{ref}^2 S. \quad (32)$$

The lift force must always at least be equal to the weight of the plane. This implies that for low speed (take-off and landing), the C_L must be large. This is accomplished with large α and slats or flaps. The minimum speed where the lift can still balance the weight (C_L maximum) is called **stall speed** and from (32) we find:

$$v_{stall} = \sqrt{\frac{W}{C_{L_{max}} \frac{1}{2} \rho_{ref} S}} \quad (33)$$

3.7 Discuss the polar curve of the airfoil, i.e. lift coefficient as a function of drag coefficient, show the glide ratio on this plot

The curve that represents C_L in function of C_D is the **polar curve** of the wing. The ratio $\frac{C_L}{C_D}$ is the **glide ratio** or **finesse** and is like an efficiency parameter.

3.8 What is the importance of the glide ratio, discuss the case of a gliding plane (engine off situation)

The best parameter is obtained using the graph by calculating β such that:

$$\tan \beta = \left(\frac{C_L}{C_D} \right)_{max} \quad (34)$$

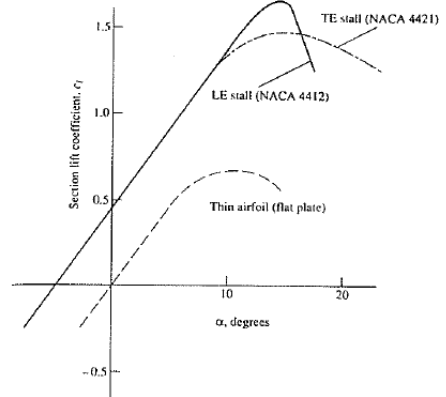


Figure 11

thick nor too thin. The figure on the left shows the influence of the thickness on the lift. We notice that the optimum thickness is situated around 12% of the chord. The maximum lift increases with Re , indeed higher the Re , higher is the ratio of speed versus viscosity. So we can better oppose to separation. Unlike the Re number, the roughness has great effects on the maximum lift. Finally, let's no-

tice that the camber have also an effect on maximum lift, the best is a camber of 8 up to 10%.

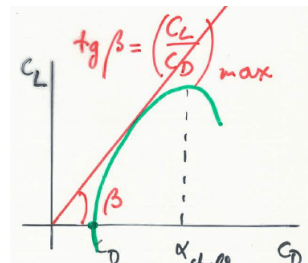


Figure 13

This point is important for the quality of the wing because if we plot the thrust, the lift, the drag and the weight of a plane describing a horizontal flight (Figure 14), the thrust is given by:

$$T = \frac{L}{\tan \beta} = \frac{W}{\tan \beta} \quad (35)$$

where we see that when $\tan \beta$ (so the glide ratio) increases, T decreases. Another interpretation can be given when we have no thrust (Figure 15). In this case the gliding ratio has to be adapted to travel the larger distance knowing that:

$$\frac{C_L}{C_D} = \frac{\text{distance travelled}}{\text{height loss}} \quad (36)$$

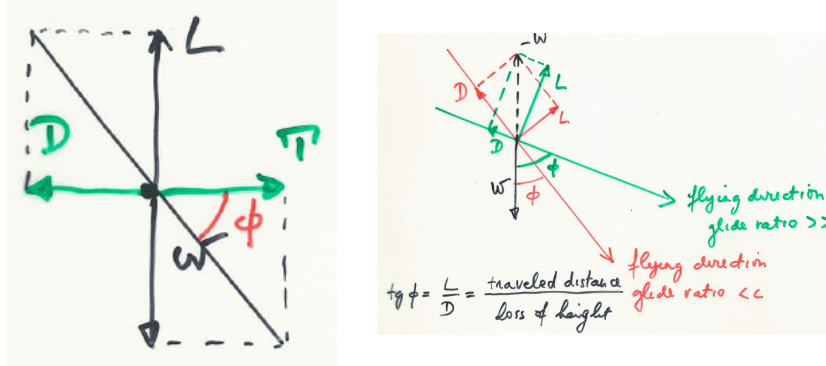


Figure 15

Figure 14

4 Computation of inviscid irrotational flow around a 2D airfoil using conformal mapping - Joukowski profiles

4.1 Explain methods based on complex potential function, explain the connection with usual stream function and potential function

We will begin here with steady, inviscid irrotational flows. This gives for the mass conservation equation:

$$\frac{\partial \rho}{\partial t} + \nabla(\rho \vec{v}) = 0 \quad \Rightarrow \nabla \vec{v} = 0 = \partial_x u + \partial_y v \quad (37)$$

In the other hand, we have the assumption of irrotational flow:

$$\vec{\omega} = 0 \quad \Rightarrow \partial_x v - \partial_y u = 0. \quad (38)$$

Then we define the **complex potential function** w:

$$w = \phi + I\psi \quad (39)$$

where ϕ is the **potential function** (satisfies $w = 0$ by construction) such that:

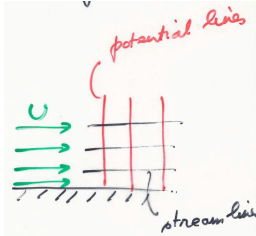
$$\begin{cases} u = \partial_x \phi \\ v = \partial_y \phi \end{cases} \quad \nabla \phi = \vec{v} = \partial_x \phi \vec{I}_x + \partial_y \phi \vec{I}_y \quad (40)$$

We must satisfy the mass conservation equation:

$$\nabla(\nabla \phi) = 0 \quad \Rightarrow \Delta \phi = 0 \quad (41)$$

coupled with boundary conditions, we can find a solution $\phi(x, y)$. The **stream function** satisfies the mass conservation by construction:

$$\begin{cases} u = \partial_y \psi \\ v = -\partial_x \psi \end{cases} \Rightarrow \partial_x u + \partial_y v = 0 \Leftrightarrow \partial_x(\partial_y \psi) + \partial_y(-\partial_x \psi) = 0 \quad (42)$$



We still have to verify the $\omega = 0$ condition:

$$\partial_x v - \partial_y u = 0 \Rightarrow \frac{\partial^2 \psi}{\partial x^2} + \frac{\partial^2 \psi}{\partial y^2} = 0 \quad \Delta \psi = 0 \quad (43)$$

A streamline and a potential line are perpendicular to each other:

$$\nabla \psi \cdot \nabla \phi = \partial_x \psi \partial_x \phi + \partial_y \psi \partial_y \phi = -v u + u v = 0. \quad (44)$$

Figure 16 means differentiable. This consist in defining a function $f(z)$ analytical such that:

$$w = f(z) \quad z, \omega \in \mathbb{C} \quad \Rightarrow w = \phi + i\psi \quad \begin{cases} z = x + iy \\ \phi = \phi(x, y) \in \mathbb{R} \\ \psi = \psi(x, y) \in \mathbb{R} \end{cases} \quad (45)$$

If this is differentiable everywhere, $\Delta \phi = \Delta \psi = 0$.

4.2 Explain how the velocity can be computed from the complex potential function

The complex velocity (velocity field):

$$\frac{dw}{dz} = \frac{df}{dz} = A + iB \quad A = \frac{\partial \phi}{\partial x} = -\frac{\partial \psi}{\partial y} = u \quad B = \frac{\partial \psi}{\partial x} = -\frac{\partial \phi}{\partial y} = -v \quad (46)$$

A property of this $f(z)$ is the superposition principle: $w_1 = f_1(z), w_2 = f_2(z)$ so $w_1 + w_2 = f_1(z) + f_2(z)$.

4.3 Derive the complex potential function for uniform flow, source/sink flow, free vortex

4.3.1 Uniform flow

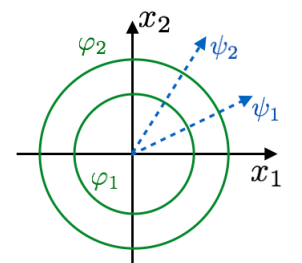
$$w = Uz \quad \frac{dw}{dz} = U = u + iv \quad \Rightarrow u = U; v = 0 \quad (47)$$

4.3.2 Source / Sink

In this case, using the cylindrical coordinates, the complex potential is defined as (Λ being the volumetric flow):

$$\begin{aligned} w &= \frac{\Lambda}{2\pi} \ln z = \frac{\Lambda}{2\pi} \ln(re^{i\theta}) = \frac{\Lambda}{2\pi} (\ln r + i\theta) \\ \Rightarrow \phi &= \frac{\Lambda}{2\pi} \ln r, \psi = \frac{\Lambda}{2\pi} \theta. \end{aligned} \quad (48)$$

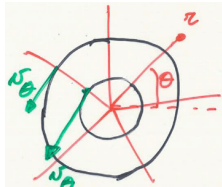
We see that complex lines corresponds to $r = cst$ so are circles and streamlines $\theta = cst$ are line of constant angle. $\oint \vec{v} d\vec{l} = 0$ as velocity is everywhere tangent to any circular contour. Let's compute the derivative for the velocity field.



$$\frac{dw}{dz} = \frac{\Lambda}{2\pi z} = \frac{\Lambda(x - iy)}{2\pi(x^2 + y^2)} = \frac{\Lambda}{2\pi r}(\cos \theta - i \sin \theta). \quad (49)$$

We see that the velocity decreases in $1/r$, this is due to the constant mass flow, so if the surface increases with r the velocity has to decrease to keep $\dot{m} = \rho v S$ constant.

4.3.3 Free vortex



We do the same as the other cases:

$$w = \frac{i\Gamma}{2\pi} \ln z = \frac{i\Gamma}{2\pi} \ln(re^{i\theta}) = \frac{i\Gamma}{2\pi} (\ln r + i\theta) = -\frac{\Gamma}{2\pi}\theta + \frac{i\Gamma}{2\pi} \ln r \quad (50)$$

$$\phi = -\frac{\Gamma}{2\pi}\theta, \psi = \frac{\Gamma}{2\pi} \ln r$$

We see that this is the inverse case of the previous one, streamlines are circles oriented in negative rotational motion around z-axis (z entering in the sheet) so clockwise. We can compute the velocity field by deriving among z and we find that:

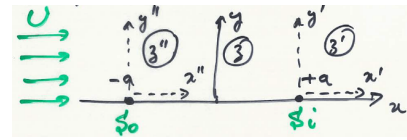
$$u = \frac{\Gamma \sin \theta}{2\pi r} \quad v = -\frac{\Gamma \cos \theta}{2\pi r} \quad (51)$$

Let's specify that $v_\theta = \frac{1}{r} \frac{\partial \phi}{\partial \theta} = -\frac{\Gamma}{2\pi r}$, and that we have a vortex singularity in the center because $\Gamma = 0.\infty$.

4.4 Compute flow around Rankine body and around a cylinder

Let's make a combination of a uniform flow and a source + sink as shown on the figure. The combination gives:

$$w = Uz + \frac{\Lambda}{2\pi} \ln \frac{z+a}{z-a} = Uz + \frac{\Lambda}{2\pi} \ln \frac{1+a/z}{1-a/z}. \quad (52)$$



To have the flow around a cylinder we need to compute the limit $a \rightarrow 0$, and will need the Taylor expansion of \ln :

$$\ln \frac{1+\epsilon}{1-\epsilon} \approx 2\epsilon + o(\epsilon^3) \quad \Rightarrow \lim_{a \rightarrow 0} w = \lim_{a \rightarrow 0} \left[Uz + \frac{\Lambda}{2\pi} 2 \frac{a}{z} \right] \quad (53)$$

by defining $\mu = 2\Lambda a$ we find the **flow around a cylinder**:

$$w = Uz + \frac{\mu}{2\pi z}. \quad (54)$$

If we replace $z = x + iy$ to find ϕ and ψ we find:

$$\phi = Ux + \frac{\mu}{2\pi} \frac{x}{r^2} \quad \psi = Uy - \frac{\mu}{2\pi} \frac{y}{r^2}. \quad (55)$$

In this flow a closed streamline exists forming the so called **Rankine body** and which describes a cylinder in the case $a \rightarrow 0$. Indeed it is possible to find an exact solution for $\psi = 0$. This configuration has a symmetry according to x and y-axis when taking the center of the cylinder as origin. This implies that $\vec{F} = -\oint_{cyl} p d\vec{S} = 0$. This is the so called **paradox of d'Alembert** because we expect to find at least a drag force. A lift force can be found on the cylinder by adding a vortex. We conclude by saying that we can rewrite (54) as (R the radius of the cylinder):

$$w = U \left(z + \frac{R^2}{z} \right) \quad \text{with } R^2 = \frac{\mu}{2\pi U}. \quad (56)$$

4.5 Explain how a the class of Joukowski profiles is obtained by conformal mapping of a circle

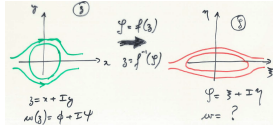


Figure 20

Let's do a mapping, a transformation, to try to find our airfoil based on simple geometries. Let's as first example apply the transformation $Z = z + \frac{R^2}{z}$ to the cylinder of radius R . Let's first remark that the cylinder will become a flat plate:

$$Z = z + \frac{R^2}{z} = Re^{i\theta} \frac{R^2}{Re^{i\theta}} = 2R \cos \theta \quad (57)$$

Indeed, as $\cos \theta \in [-1, 1]$ and the result is real, we have a flat plate between $-2R$ and $2R$ in the x -axis. The flow Z is directly found: $W(Z) = UZ$. The second example will be the application of the same transformation on a cylinder of this time radius $r > R$. In this case the circle becomes an ellipse:

$$Z = re^{i\theta} + \frac{R^2}{r^2} e^{-i\theta} = \left(r + \frac{R^2}{r}\right) \cos \theta + i \left(r - \frac{R^2}{r}\right) \sin \theta. \quad (58)$$

Let's also compute the velocity field using the chain rule:

$$\frac{dW}{dZ} = \frac{dw}{dZ} = \frac{dw}{dz} \frac{dz}{dZ} = \left(1 - \frac{r^2}{z^2}\right) \left(\frac{1}{1 - \frac{R^2}{z^2}}\right). \quad (59)$$

We see that the expression becomes infinite when $z^2 = R^2$. The reason is that the transformation is not analytical in these points so they must not be in the flow.

The examples are summarized in the figures below

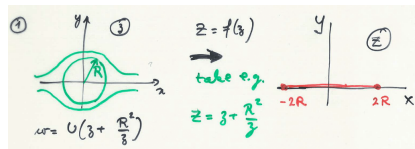


Figure 21

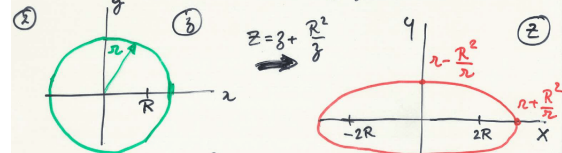


Figure 22

Now suppose that we place no longer the center of the cylinder at the origin, but on the real axis. The mapping of the cylinder now takes the shape of a **symmetrical wing profile**. We see that there are two remarkable points that are H and A corresponding to the points H_1 and A_1 of the black and red circles, our profile is in between them. Now to give camber we only have to move the center of the cylinder on the y -axis. Please reffer to figures below.

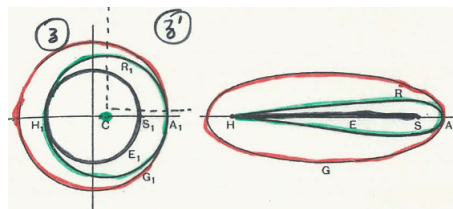


Figure 23

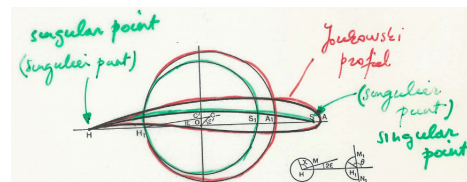


Figure 24

Note that for the green circle in first figure, the complex potential becomes:

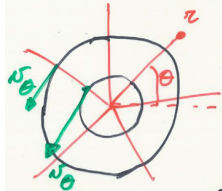
$$w = U \left(z - z_c + \frac{r^2}{z - z_c} \right) \quad (60)$$

As last remark, let's remind that we had singularities in the second example. These points corresponds here to H_1 and S_1 . The mapping of H_1 is always H the trailing edge, the velocity is there infinitely large. This was the discussion we've previously done with the stagnation point that has to move on the trailing edge otherwise $v = \infty$ because of the sharp edge. We can solve this by adding a vortex. This methods gives a limited amount of airfoils.

5 Computation of inviscid irrotational flow around a thin airfoil based on a continuous distribution of vortices

5.1 Explain what is a free vortex

A free vortex is an irrotationnal vortex where the flow velocity u is inversely proportional to the distance r .



Streamlines are circles oriented in negative rotational motion around z-axis (z entering in the sheet) so clockwise. We can compute the velocity field by deriving among z and we find that:

$$u = \frac{\Gamma \sin \theta}{2\pi r} \quad v = -\frac{\Gamma \cos \theta}{2\pi r} \quad (61)$$

Figure 25

Let's specify that $v_\theta = \frac{1}{r} \frac{\partial \phi}{\partial \theta} = -\frac{\Gamma}{2\pi r}$, and that we have a vortex singularity in the center because $\Gamma = 0.\infty$.

5.2 Explain what is a continuous distribution of free vortices on a line

A way to represent thin airfoils is to use only their camberline and to retrieve the flow using an infinite line of free vorticities (or sources). A infinite line of vorticities thus represents an infinite thin airfoil.

5.3 Explain principle of the method of free vortex distribution applied thin airfoils, limitations and hypotheses

We will suppose infinitely thin airfoil and small angle of attack, so that the airfoil is represented by the camber line. This means also small camber about 2-3% of the chord and $\alpha < 8\%$. We can try to retrieve the flow by superposition principle by using infinite number of elementary sources or elementary vorticities. The potential function for the sources is:

$$\phi = \frac{\Lambda}{2\pi} \ln r \quad d\phi = \frac{d\Lambda}{2\pi} \ln r \quad (62)$$

We then describe the source distribution by the source intensity $\lambda = \frac{d\Lambda}{ds}$ on a part ds of the wing so that the last equation becomes:

$$d\phi = \frac{\lambda}{2\pi} \ln r ds. \quad (63)$$

We will use the second method presented now which is using the vorticities:

$$\phi = -\frac{\Gamma}{2\pi}\theta \quad \vec{v} = \nabla\phi = \underbrace{\frac{\partial\phi}{\partial r}\vec{1}_r}_{=v_r=0} + \underbrace{\frac{1}{r}\frac{\partial\phi}{\partial\theta}\vec{1}_\theta}_{=v_\theta} \Rightarrow v_\theta = -\frac{\Gamma}{2\pi}\frac{1}{r}. \quad (64)$$

In the same way as the other we can define a **vortex intensity** to characterize the vortex distribution on a part ds $\gamma = \frac{d\Gamma}{ds}$, the derivative of ϕ and the elementary velocity are then:

$$d\phi = -\frac{\gamma}{2\pi}\theta ds \quad dv_\theta = -\frac{\gamma ds}{2\pi r}. \quad (65)$$

The aim now is to make that infinitely thin airfoil a streamline. We assume because of superposition that the flow is a uniform flow \vec{U}_∞ , that we have an angle of attack α . Because of the vortices, we have a velocity perturbation \vec{v} such that the total velocity is:

$$\vec{V}_\infty = \vec{U}_\infty + \vec{v}. \quad (66)$$

5.4 Establish the integral equation which allows to compute the vortex distribution for a given profile

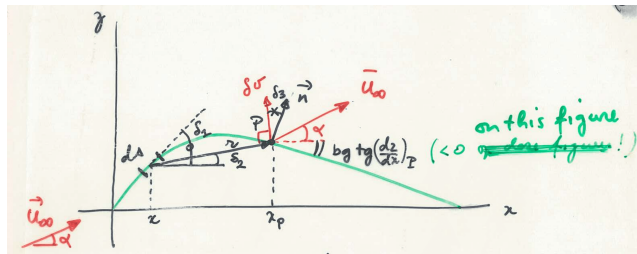


Figure 26

We must now choose γ such that \vec{V} is tangential to the airfoil everywhere (we want the camber line to be a streamline). In other words, $\forall P$ the normal component of the velocity should be null $V_{nP} = U_{\infty nP} + v_{nP} = 0$. Let's determine these components by projection. First, for $U_{\infty nP}$ we can remark the sum of angle α and the camber line slope $\tan\beta = \left(-\frac{dz}{dx}\right)_P \Rightarrow \beta = -\arctan\left(\frac{dz}{dx}\right)_P$, the projection is (camber line: $z = f(x)$):

$$U_{\infty nP} = U_\infty \sin \left[\alpha - \arctan \left(\frac{dz}{dx} \right)_P \right]. \quad (67)$$

Now for v_{nP} , we consider an elementary vortex on a point x on the airfoil that creates an elementary perturbation δv_n on point P . This velocity direction is θ in a (r, θ) axis with origin at x , so perpendicular to r on the figure. If the angle with the normal is δ_3 , the projection will be:

$$\delta v_n = -\frac{\gamma(x)ds}{2\pi r} \cos \delta_3. \quad (68)$$

Now we have infinite number of contribution of the infinite vortices, as γ, r and δ_3 depend on position P , we have to integrate over the whole airfoil:

$$v_n = -\frac{1}{2\pi} \int_0^c \frac{\gamma(x)ds}{r} \cos \delta_3 \quad (69)$$

where c is the chord length. We can express both r and ds in function of x as:

$$r = \frac{x_P - x}{\cos \delta_2} \quad ds = \frac{dx}{\cos \delta_1} \quad (70)$$

which gives

$$v_n = -\frac{1}{2\pi} \int_0^c \frac{\gamma(x)dx}{x_P - x} \frac{\cos \delta_2}{\cos \delta_1} \cos \delta_3. \quad (71)$$

We are able to reconsider the condition (67) by replacing our results:

$$\frac{1}{2\pi} \int_0^c \frac{\gamma(x)dx}{x_P - x \cos \delta_1} \cos \delta_3 = U_\infty \sin \left[\alpha - \arctan \left(\frac{dz}{dx} \right)_P \right]. \quad (72)$$

This is a relatively complicated equation, we can simplify it by **assuming a small camber** (in practice 2% of the chord), which allows to say that $\delta_1 \approx \delta_2 \approx \delta_3 \approx 0$ and $\arctan \left(\frac{dz}{dx} \right)_P = \left(\frac{dz}{dx} \right)_P$. By considering α small, $\sin \alpha \approx \alpha$:

$$\frac{1}{2\pi} \int_0^c \frac{\gamma(x)dx}{x_P - x} = U_\infty \left[\alpha - \left(\frac{dz}{dx} \right)_P \right]. \quad (73)$$

We will introduce a new variable θ , considering $x = \frac{1}{2}c(1 - \cos \theta)$ and $dx = \frac{1}{2}c \sin \theta d\theta$:

$$\frac{1}{2\pi} \int_0^\pi \frac{\gamma(\theta) \sin \theta d\theta}{\cos \theta - \cos \theta_P} = U_\infty \left[\alpha - \left(\frac{dz}{dx} \right)_P \right]. \quad (74)$$

5.5 Show how to solve this equation using a spectral method, i.e. by expressing the vortex distribution as a truncated Fourier series

Let's express $\gamma(\theta)$ in series:

$$\gamma(\theta) = 2U_\infty \left(A_0 \coth \frac{\theta}{2} + \sum_{n=1}^{\infty} A_n \sin(n\theta) \right). \quad (75)$$

This is in fact a solution of the last equation.

Now we can replace this definition on the previous equation, knowing that $\coth(\theta/2) \sin \theta = 1 + \cos \theta$ and writing $\theta_P = \theta'$, we get:

$$\frac{1}{2\pi} \int_0^\pi \frac{\gamma(\theta) \sin \theta d\theta}{\cos \theta - \cos \theta'} = \frac{U_\infty}{\pi} \left[\int_0^\pi \frac{A_0(1 + \cos \theta) d\theta}{\cos \theta - \cos \theta'} + \sum_n A_n \int_0^\pi \frac{\sin(n\theta) \sin \theta d\theta}{\cos \theta - \cos \theta'} \right] \quad (76)$$

By using the equality here and the **Glauert integral**:

$$\sin(n\theta) \sin \theta = -\frac{1}{2} [\cos((n+1)\theta) - \cos((n-1)\theta)] \quad \int_0^\pi \frac{\cos(n\theta) d\theta}{\cos \theta - \cos \theta'} = \pi \frac{\sin(n\theta')}{\sin \theta'} \quad (77)$$

The integral becomes:

$$\frac{U_\infty}{\pi} \left[A_0 \cdot 0 + A_0 \cdot \pi - \frac{\pi}{2} \sum_n A_n \frac{\sin((n+1)\theta') - \sin((n-1)\theta')}{\sin \theta'} \right] = U_\infty \left[A_0 - \sum_n A_n \cos(n\theta') \right] \quad (78)$$

where we used the Simpson equation. The (74) becomes:

$$A_0 - \sum_n A_n \cos(n\theta') = \alpha - \left(\frac{dz}{dx} \right)' \quad (79)$$

This equation must be valid $\forall P$ on the airfoil. To find the coefficients A_i , let's integrate first this for $0 \leq \theta' \leq \pi$ in order to compute A_0 :

$$A_0\pi - \sum_n A_n \int_0^\pi \cos(n\theta') d\theta' = \alpha\pi - \int_0^\pi \frac{dz}{dx} d\theta \Rightarrow A_0 = \alpha - \frac{1}{\pi} \int_0^\pi \frac{dz}{dx} d\theta. \quad (80)$$

For the A_n , we multiply the same equation by $\cos(m\theta')$ before integrating (we will drop the $'$). Let's see that $\int_0^\pi \cos(n\theta) \cos(m\theta) d\theta = 0$ if $m \neq n$ and $= \pi/2$ if $n = m$. We finally get:

$$A_n = \frac{2}{\pi} \int_0^\pi \frac{dz}{dx} \cos(m\theta) d\theta. \quad (81)$$

We can note that for A_n only the camber plays a role, the angle of attack does not appear. Only A_0 is influenced by α . We are now able to compute any vorticity distribution $\gamma(\theta)$, for example for a flat plate $A_n = 0$ and $A_0 = \alpha$.

5.6 How is the Kutta-Youkowsky condition imposed (allowing to compute the lift)

The above respects the Kutta condition that states that there is no vortex allowed on the trailing edge. Indeed, $\gamma(\pi) = 0$ which means no contribution by vortex. We can also state that at the leading edge, the stagnation point is in the pressure side at the front. Indeed, for $\theta = 0$, $\coth \theta = \infty = \gamma(\pi)$ which means that we have a singularity at the TE and that the velocity is infinite due to the turning on the LE.

5.7 Starting from the expressions for the Fourier coefficients, compute the circulation and lift coefficient as a function of angle of attack, explain the result

5.7.1 Calculation of the total circulation

To get Γ we only have to compute the integral over the whole airfoil:

$$\begin{aligned} \Gamma &= \int_0^c \gamma(x) dx = \frac{1}{2} c \int_0^\pi \gamma(\theta) \sin \theta d\theta \\ &= \frac{1}{2} c \left[2U_\infty \int_0^\pi A_0(1 + \cos \theta) d\theta + 2U_\infty \sum_{n=1}^{\infty} \int_0^\pi A_n \sin(n\theta) \sin \theta d\theta \right] \\ &= U_\infty c \left[A_0\pi + 2U_\infty + \int_0^\pi \sin^2(\theta) d\theta - \frac{1}{2} \sum_{n=2}^{\infty} \int_0^\pi A_n \cos[(n+1)\theta - \cos(n-1)\theta] d\theta \right] \\ &= U_\infty c[A_0\pi + A_1\pi/2]. \end{aligned} \quad (82)$$

We see that the circulation only depends on two coefficients.

5.7.2 Calculation of the lift coefficient

We can now compute the lift using the kutta formula $L = \rho_\infty U_\infty \Gamma$. We are interested in the c_l and not the lift itself. In 2D we have to divide by the chord so:

$$c_l = \frac{L}{\frac{1}{2} \rho_\infty U_\infty^2 C} = \frac{2\Gamma}{U_\infty c} = \pi(2A_0 + A_1) \quad (83)$$

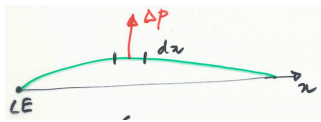
We can now replace by definition of the coefficients:

$$c_l = 2\pi \left(\alpha - \underbrace{\frac{1}{\pi} \int_0^\pi \frac{dz}{dx} (1 - \cos \theta) d\theta}_{\alpha_0} \right) = 2\pi(\alpha - \alpha_0) \quad (84)$$

where α_0 is the **zero lift angle of attack**. We see that we have a linear relation with respect to α . We have the theoretical model the same for every profile, only α_0 changes with the profile. Remark that the lift is also the integral of the pressure on the lower and upper side:

$$L = \int_0^c (p_l - p_u) dx = \rho_\infty U_\infty \int_0^c \gamma dx \quad \Rightarrow p_l - p_u = \rho_\infty U_\infty \gamma(x). \quad (85)$$

5.8 Starting from the expression for the momentum coefficient at the leading edge $c_m(\text{LE})$, show that it's a linear function of the lift coefficient c_l



The contribution of the elementary parts of the airfoil gives:

$$\begin{aligned} dM_{LE} &= -(\Delta p dx)x \\ \Rightarrow M_{LE} &= - \int_0^c \Delta p x dx = -\rho_\infty U_\infty \int_0^c \gamma x dx \end{aligned} \quad (86)$$

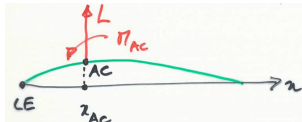
Figure 27

After some manipulations (not detailed):

$$c_{m_{LE}} = \frac{M_{LE}}{\frac{1}{2} \rho_\infty U_\infty^2 c^2} = -\frac{\pi}{4} (2A_0 + 2A_1 - A_2) = -\frac{1}{4} c_l - \frac{\pi}{4} (A_1 - A_2) \quad (87)$$

where we used (83) for the last expression.

5.9 Compute the location of the aerodynamic center AC and the momentum coefficient in the aerodynamic center



The moment on the LE is related to the moment anywhere:

$$M_{LE} = M_{ac} - x_{ac} L \quad \Rightarrow c_{m_{LE}} = c_{m_{ac}} - \frac{x_{ac}}{c} c_l \quad (88)$$

By using the last result of the previous section, we get:

Figure 28

$$c_{m_{ac}} = \left(\frac{x_{ac}}{c} - \frac{1}{4} \right) c_l - \frac{\pi}{4} (A_1 - A_2). \quad (89)$$

We see that, for this relation to be independent of the angle of attack, we must have $x_{ac} = \frac{c}{4}$ so that:

$$c_{m_{ac}} = \frac{\pi}{4} (A_2 - A_1). \quad (90)$$

Remark that for symmetrical wings $\frac{dz}{dx} = 0 \Rightarrow A_1 = A_2 = 0 \Rightarrow c_{m_{ac}} = 0$.

5.10 Compute the location of the center of pressure

The formula used in the previous section is valid, we replace ac by cp, and since the moment should be null at this point:

$$c_{m_{cp}} = c_{m_{LE}} + \frac{x_{cp}}{c} c_l = 0 \quad \Rightarrow \frac{x_{cp}}{c} = \frac{1}{4} + \frac{\frac{\pi}{4} (A_1 - A_2)}{c_l} = \frac{1}{4} - \frac{c_{m_{ac}}}{c_l}. \quad (91)$$

Some remarks:

- the center of pressure is not fixed and varies with the lift
- at 0 lift, $x_{cp} \rightarrow \infty$ (for symmetric wing $x_{cp} = x_{ac} = c/4$ fixed)
- cp always downstream to ac because $c_{m_{ac}} < 0$.

6 Computation of inviscid irrotational flow around a thin airfoil based on a continuous distribution of vortices

Discuss the influence of a flap located at the trailing edge of the airfoil According to the definition of the zero lift angle in (84), the effect of the shape becomes greater when $\theta \approx 180^\circ$ (trailing edge). By making the zero lift angle more negative we can produce more lift before the critical angle of attack that decreases a bit.

The effect is evaluated by taking a flat plate as camber line with a deflection near the TE, starting at E% of the chord and slope η . E in function of θ_E is:

$$E = \frac{1}{2}(1 + \cos \theta_E). \quad (92)$$

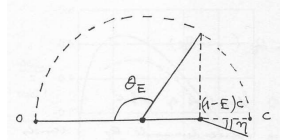


Figure 29

In this case, A_0 and A_n can be rewritten as:

$$\begin{aligned} A_0 &= \alpha - \frac{1}{\pi} \int_0^\pi \frac{dz}{dx} d\theta \approx \alpha - \frac{\eta}{\pi}(\pi - \theta_E) \\ A_n &= \frac{2}{\pi} \int_0^\pi \frac{dz}{dx} \cos(n\theta) d\theta \approx -\frac{2\eta}{\pi n} \sin(n\theta_E) \end{aligned} \quad (93)$$

such that the lift coefficient becomes:

$$c_l = \pi(2A_0 + A_1) = \underbrace{2\pi\alpha}_{\text{without flaps}} \underbrace{-2\eta(\pi - \theta_E + \sin \theta)}_{\Delta c_l > 0 \text{ since } \eta < 0}. \quad (94)$$

This seems to be like $c_l = 2\pi(\alpha - \alpha_0)$ allowing the definition for the zero lift angle:

$$\alpha_0 = \frac{\eta}{\pi}(\pi - \theta_E + \sin \theta) \quad (95)$$

which indicates an increase (decrease since $\eta < 0$) of α_0 since it is null for the flat plate. For the moment at the ac (90)

$$\Delta c_{m_{ac}} = \frac{\eta}{2} \sin \theta_E (1 - \cos \theta_E) \quad (96)$$

which also indicates a decrease in the momentum which is 0 for the symmetric wing.

Determine the effect of the flap on:

the lift curve: from the above, we see that lift goes up with flaps

the zero lift angle of attack: It is increased, see above

the moment at the aerodynamic center: It decreases.

7 3D wing theory

7.1 Explain mean chord, span, aspect ratio, taper, sweep of wing

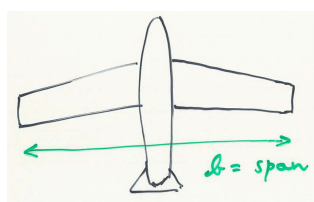


Figure 30

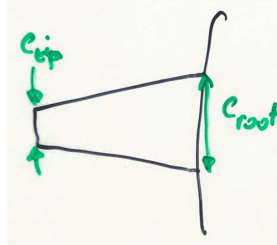


Figure 31

The **span** is the total distance between the tips of the wings, plane body included. It is a straight line.

The **mean chord** is defined by dividing the wing area by the span. This is used to avoid having a chord that varies for calculations.

The **aspect ratio** is the span divided by the mean chord, or the span squared divided by the wing surface. Higher aspect ration means higher lift to drag ratio.

Tapered wings are wing that have a bigger chord near the body. The **taper ratio** is defined by $\frac{c_{tip}}{c_{root}}$

Swept wings are wings that are (at least partially) not \perp to the flow. This is to delay shock wave formation. The sweep is the angle of the leading and/or trailing edge compared to the \perp to the flow.

7.2 Explain downwash effect, downwash angle, effective angle of attack, total and induced drag

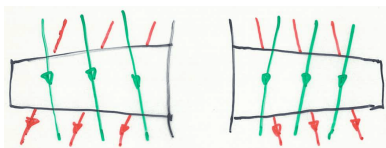


Figure 32

Finite span \Rightarrow the pressure on both side must be equal at the end of the span. This means that the pressure on the upper side must increase when going to the tip, and decrease on the lower side. This creates a pressure gradient between the root and the tip. This gradient will push the streamlines on the upper side towards the fuselage and towards the tip on the lower side.



Figure 33



Figure 34

Looking from downstream, this discontinuity in velocity induces an infinite series of infinitely small vortices, clockwise on the left and anti clockwise on the right wing (Figure 33), resulting in 2 discrete vortices at the tip, the **swung-tip vortices or trailing vortices** (Figure 34).

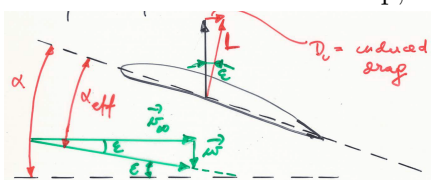


Figure 35

These vortices induce a **downward velocity component**, the **downwash** \vec{w} . This component superposes on the incoming flow and changes the angle of attack (Figure 35). The angle of change is the **downwash angle**, or induced angle of attack and we compute the **effective angle of attack** $\alpha_{eff} = \alpha - \epsilon$ where ϵ is the induced angle of attack.

The decrease of α means a decrease in lift as the new lift is perpendicular to the new flow, some of it's force produces an **induced drag**.

The **total drag** C_D is computed as being the sum of the profile drag and the induced one. (in reality, we also have to take into account the parasite drags created by the fuselage, antennas,...)

7.3 Starting from the given expression for the downwash angle, compute the induced drag force and the induced drag coefficient

$$\alpha_{eff} = \alpha - \epsilon \quad (97)$$

induced drag:

$$D_i = L \sin \alpha_i \approx L \alpha_i \quad \text{with} \quad \alpha_i = \frac{C_L}{\pi e A R} \quad (98)$$

where e is the **span efficiency factor or Oswald's efficiency factor** $0.85 < e < 1$. We get the Drag coefficient:

$$C_{D_i} = \frac{C_L^2}{\pi e A R}. \quad (99)$$

7.4 Explain the lift curve as a function of the angle of attack for a 3D wing, compare with the lift curve for a 2D profile

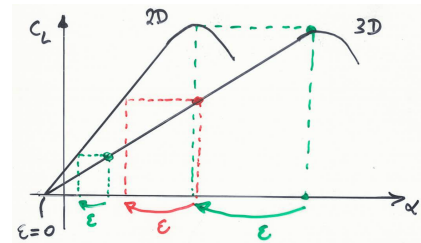


Figure 36

The theoretical lift curve can be obtained based on the 2D wing as Figure 36. We can see that the 3D wing lift for a certain α corresponds to the 2D lift for the effective angle of attack $\alpha - \epsilon$. The induced angle of attack decreases with lift, at α_0 the two curve are on the same point. Algebraically the 2D and 3D curves can be noted:

$$c_l = m(\alpha - \alpha_0), \quad C_L = m(\alpha - \epsilon - \alpha_0) = m^*(\alpha - \alpha_0) \quad (100)$$

where m^* is the slope of the 3D lift. We can isolate this and find that:

$$m^* = m \left(1 - \frac{\epsilon}{\alpha - \alpha_0} \right) = \frac{m}{1 + \frac{m}{\pi e A R}} \quad (101)$$

where we used the definition (98) and (100) for the last result. We see that the slope is independent from α .

7.5 Give the expression for the total drag coefficient as a function of C_L

The total drag is the sum of the profile drag and the induced one:

$$C_D = C_{D_0} + k C_L^2 + C_{D_i} = C_{D_0} + C_L^2 \left(k + \frac{1}{\pi e A R} \right) \quad (102)$$

where k is generally small compared to the other.

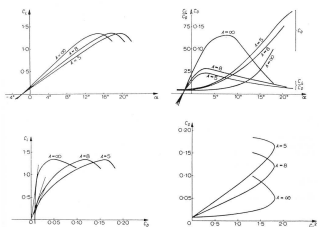


Figure 37

With these formulas we can plot the characteristics in 3D. We can note that the maximum lift does not change so much, but there is a strong decrease in the maximum glide ratio, C_D increases with C_L so α . Finally we note an increase of the stall angle but in practice this is not as large as predicted. This means also that the maximum lift decreases

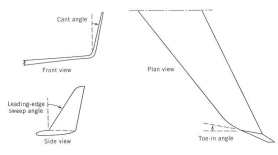


Figure 38

slightly with decreasing AR. No significant difference for the moment.

To avoid the adverse effect which is increasing induced drag. We can use high AR or add winglet on the tip, a kind of end plate that forces a vertical diffusion of the tip vortex, reducing drag. They have to be carefully designed to not increase the viscous drag.

7.6 Give the expression of the drag force D as a function of the velocity at infinity

Let's compute the total drag using the coefficient definition:

$$D = C_D \frac{1}{2} \rho_\infty v_\infty^2 S = C_{D_0} \frac{1}{2} \rho_\infty v_\infty^2 S + \left(k + \frac{1}{\pi e A R} \right) \frac{L^2}{(\frac{1}{2} \rho_\infty v_\infty^2 S)^2} \frac{1}{2} \rho_\infty v_\infty^2 S \\ = k_1 v_\infty^2 + k_2 v_\infty^2. \quad (103)$$

8 3D wing theory – Derivation of Prandtl lifting line method Give the basic ideas and the development of Prandtl's lifting line theory

8.1 Velocity induced by a vortex filament

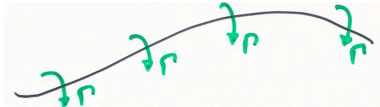


Figure 39

The seen free vortex is characterized by circular streamlines around a certain point P. In this point the vorticity is concentrated such that the circulation around the contours that don't contain the point are null. If we consider several planes above each other containing a 2D free vortex, the point P

form a line called **vortex line** or **vortex filament**. The circulation on each point of that line have the same circulation.



Figure 40

This line can be a random line with bending. Now if one places an infinite number of vortex lines besides each other, we get a **vortex sheet**.

The normal component of the velocity is continuous while the tangential one varies as $\Delta v_t = \gamma$ with gamma given by the circulation around a vortex sheet.

Using Bio-Savart at point P:

$$\vec{v} = \frac{\Gamma}{4\pi} \int_{-\infty}^{+\infty} \frac{d\vec{l} \times \vec{r}}{|r|^3}. \quad (104)$$

We have: $d\vec{l} \times \vec{r} = R d\vec{l} \vec{l}_n$, $\vec{v} = v \vec{l}_n$ (see figure). Let's define the length l beginning from the piercing point on the surface until the $d\vec{l}$. We can graphically see that:

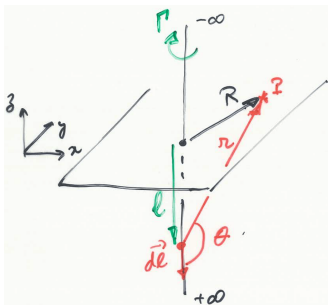


Figure 41

$$l = -R \coth \theta \Rightarrow dl = \frac{R}{\sin^2 \theta} d\theta, \quad r = \frac{R}{\sin \theta} \quad (105)$$

Replacing all this we get:

$$v = \frac{\Gamma}{4\pi} \int_0^\pi \frac{R^2}{\sin^2 \theta} \frac{\sin^3 \theta}{R^3} d\theta \Rightarrow v = \frac{\Gamma}{2\pi R}. \quad (106)$$

This is the velocity distribution of the 2D free vortex.

8.2 Helmholtz theorems, Biot-Savart law

Helmholtz theorems

- Along a vortex line, the circulation must be constant.
- A vortex line cannot finish in the flow but must continue to the edges of the flow or form a closed contour.

This law gives the induced velocity in a certain point P caused by an elementary piece $d\vec{l}$ of the filament:

Law of Biot-Savart

$$d\vec{v} = \frac{\Gamma}{4\pi} \frac{d\vec{l} \times r}{|r|^3} \quad (107)$$

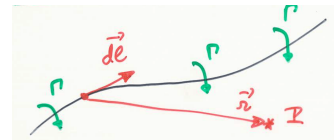


Figure 42

With analogy to electrical wire where we have a current intensity that induces a magnetic field on point P: $d\vec{B} = \frac{\mu I}{4\pi} \frac{d\vec{l} \times r}{|r|^3}$.

8.3 Circulation around a vortex sheet

For the total circulation to be finite, the circulations must be infinitely small, but can vary from one line to the other. The circulation of the vortex sheet is calculated as:

$$\Gamma = \int_a^b d\Gamma = \gamma ds \quad (108)$$

8.4 Downwash velocity induced by a single horseshoe vortex, why this model for a wing is not working

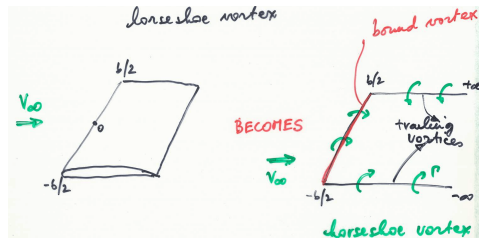


Figure 43

The idea is to represent the 3D wing by means of vortex filaments. On the figure we have the **horseshoe vortex** where the x direction continues to infinity to satisfy the Helmholtz condition and the y direction extends from $-b/2$ to $b/2$ and represents the two wings. This last is the bound vortex and the one in x direction represents the tip vortices. The problem with the representation is that we have a constant circulation while we have seen that the lift decreases when going to the tips.

Let's try to compute the downwash velocity on a point from the bound vortex. The law of Biot-Savart has 3 contributions:

$$\vec{v} = \int_{-\infty}^{-b/2} \dots + \int_{-b/2}^{b/2} \dots + \int_{b/2}^{\infty} \dots \quad (109)$$

The second integral vanishes as dl and r are parallel, the two others were computed at the previous section. Pay attention

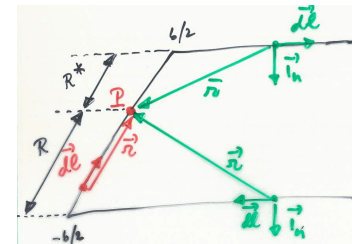


Figure 44

that we have to take half the contribution as the integral is not $-\infty, +\infty$:

$$\vec{v}(y) = \left(\frac{\Gamma}{4\pi R} + \frac{\Gamma}{4\pi R^*} \right) \vec{l}_n \quad (110)$$

We can see that the velocity is infinity at the tips and minimum at the middle. This is clearly not the reality.

8.5 Downwash velocity induced by a superposition of horseshoe vortices

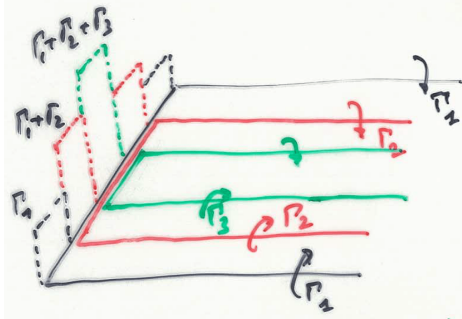


Figure 45

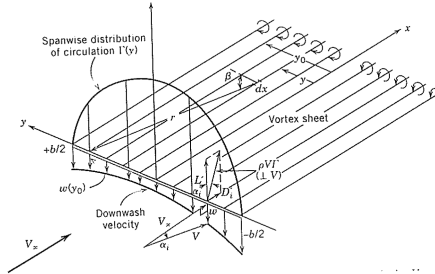


Figure 46

The solution is to superpose the horseshoes with bound vortices with different length (fig:Figure 45). If now we let tend the number of superimposed horseshoe vortices to infinity, we will get a vortex sheet as represented on Figure 46. The continuously varying circulation on the wing is no longer constant and this corresponds better with the reality.

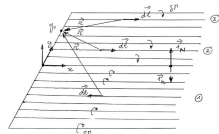


Figure 47

Consider this figure, we will try to compute the downwash velocity by considering a large but finite number of vortices of circulation $d\Gamma$ for each. We have 3 regions to consider with our basic formula:

- $y < 0: d\vec{v}(y_0) = \frac{d\Gamma}{4\pi(y_0-y)} \vec{l}_n$
- $0 < y < y_0: d\vec{v}(y_0) = \frac{d\Gamma}{4\pi(y_0-y)} \vec{l}_N = \frac{-d\Gamma}{4\pi(y_0-y)} \vec{l}_n$
- $y_0 < y: d\vec{v}(y_0) = \frac{d\Gamma}{4\pi(y-y_0)} \vec{l}_n = \frac{-d\Gamma}{4\pi(y-y_0)} \vec{l}_n$

We can see that the three formulas are the same if we take $\Gamma < 0$ for $y > 0$. We can so write the total contribution and its extension to the infinite number of lines:

$$\vec{v} = \left[\sum \frac{d\Gamma}{4\pi(y_0-y)} \right] = \left[\int_{-b/2}^{b/2} \frac{d\Gamma}{4\pi(y_0-y)} \right] \quad (111)$$

8.6 Derivation of Prandtl's fundamental equation of lifting line theory

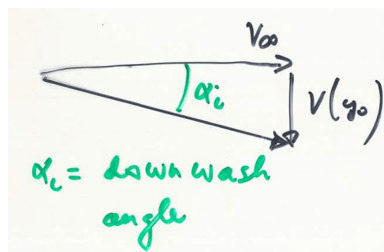


Figure 48

The induced angle of attack is then given by:

$$\tan \alpha_i \approx \alpha_i = \frac{v(y_0)}{v_\infty} = \frac{1}{4\pi v_\infty} \int_{-b/2}^{b/2} \frac{d\Gamma}{y_0 - y}. \quad (112)$$

Now let's denote $\alpha_{eff} = \alpha - \epsilon$. We know that the theory says $c_l = 2\pi(\alpha_{eff}(y_0) - \alpha_0(y_0))$, and using the definition of c_l and the Kutta-Jukowski for $L(y_0)$ we get:

$$c_l = \frac{L(y_0)}{\frac{1}{2}\rho_\infty v_\infty^2 c(y_0)} = \frac{\rho_\infty v_\infty \Gamma(y_0)}{\frac{1}{2}\rho_\infty v_\infty^2 c(y_0)} = \frac{\Gamma(y_0)}{\frac{1}{2}v_\infty^2 c(y_0)}$$

$$\Rightarrow \alpha_{eff} = \frac{\Gamma(y_0)}{\pi v_\infty c(y_0)} + \alpha_0(y_0)$$
(113)

Combining all the result, we can compute the α :

Fundamental equation of Prandtl's lifting line theory

$$\alpha(y_0) = \frac{\Gamma(y_0)}{\pi v_\infty c(y_0)} + \alpha_0(y_0) + \frac{1}{4\pi v_\infty} \int_{-b/2}^{b/2} \frac{d\Gamma}{y_0 - y}. \quad (114)$$

The only unknown in this equation is the circulation: several cases.

9 3D wing theory: application of Prandtl lifting line theory for a wing with given circulation Starting from Prandtl's fundamental equation of lifting line theory and the formula for the induced angle of attack:

Fundamental equation of Prandtl's lifting line theory

$$\alpha(y_0) = \frac{\Gamma(y_0)}{\pi v_\infty c(y_0)} + \alpha_0(y_0) + \frac{1}{4\pi v_\infty} \int_{-b/2}^{b/2} \frac{d\Gamma}{y_0 - y}. \quad (115)$$

$$\tan \alpha_i \approx \alpha_i = \frac{v(y_0)}{v_\infty} = \frac{1}{4\pi v_\infty} \int_{-b/2}^{b/2} \frac{d\Gamma}{y_0 - y}. \quad (116)$$

9.1 Discuss the different terms of the equation

Γ is the circulation around the vortex sheet, v_∞ the flow speed, $c(y_0)$ the point where we calculate the downwash, y the position of a vortex wire. (see graphs above)

9.2 Apply to a wing with a given circulation distribution: find lift and drag coefficients

Idea is to solve the integral. The discussions below do it for more complicated case, so good luck!

9.3 Apply to a wing with a given shape and unknown circulation distribution defined by a truncated Fourier series and compute the lift C_L and the induced drag C_{Di} coefficients

Local and total lift by:

$$L'(y_0) = \rho_\infty v_\infty \Gamma(y_0) \quad L = \int_{-b/2}^{b/2} L'(y) dy \quad (117)$$

and the local and total induced drag:

$$D'_i(y_0) = \Gamma(y_0)\epsilon(y_0) \quad D_i = \int_{-b/2}^{b/2} D'_i(y) dy \quad (118)$$

We assume a serie:

$$\Gamma = \sum_{n=1}^N A_n \sin(n\theta). \quad (119)$$

Substitution of this in the Prandtl's fundamental equation gives:

$$\alpha(\theta_0) = \frac{1}{\pi v_\infty c(\theta_0)} \sum_n A_n \sin(n\theta_0) + \alpha_0(\theta_0) + \frac{1}{2\pi v_\infty b} \sum_n A_n n \int_\pi^0 \frac{\cos(n\theta)d\theta}{\cos\theta_0 - \cos\theta} \quad (120)$$

→ Glauert integral. We can find a solution by considering N equations for N points distributed along the span.

By integration of the local lift and definition of C_L and C_D :

$$C_L = \frac{1}{\frac{1}{2}v_\infty S} \int_{-b/2}^{b/2} \Gamma(y) dy = \frac{b}{u_\infty S} \sum_n \int_0^\pi A_n \sin(n\theta) \sin\theta d\theta = \frac{\pi b A_1}{2S v_\infty}. \quad (121)$$

$$C_{D_i} = \frac{1}{\frac{1}{2}v_\infty S} \int_{-b/2}^{b/2} \Gamma(y) \alpha_i dy. \quad (122)$$

Using (116), we can express $\alpha_i(\theta_0)$ as:

$$\alpha_i(\theta_0) = \frac{1}{2\pi v_\infty b} \int_\pi^0 \frac{\frac{d\Gamma}{d\theta}}{\cos\theta_0 - \cos\theta} d\theta = \frac{1}{2\sin\theta_0 v_\infty b} \sum_n A_n n \sin(n\theta_0) \quad (123)$$

which gives:

$$C_{D_i} = \frac{1}{2v_\infty^2 S} \int_0^\pi \sum_n \sum_k A_n A_k \sin(n\theta) \sin(k\theta) d\theta = \frac{\pi}{4v_\infty^2 S} \sum_n A_n^2 n \quad (124)$$

and using the lift coefficient:

$$C_{D_i} = \frac{C_L^2}{\pi AR} \left(1 + \sum_{n=2} \left(\frac{A_n}{A_1} \right)^2 \right) \Rightarrow e = \frac{1}{1 + \sum_{n=2} \left(\frac{A_n}{A_1} \right)^2} = \frac{1}{1 + \delta} \quad (125)$$

where δ is the **induced drag factor**, since it is always positive, $e < 1$.

9.4 Apply to a tapered wing



Figure 49



Figure 50

Same 2D profile along the span and no twist. Because of the symmetry, it is obvious that the pair n in the series will have no contribution. Let's go until 7:

$$\Gamma = A_1 \sin\theta + A_3 \sin 3\theta + A_5 \sin 5\theta + A_7 \sin 7\theta. \quad (126)$$

To determine the coefficient we have to apply (120) to 4 points. Let's take half the span because of symmetry: $\theta = \pi/8, \pi/4, 3\pi/8, \pi/2$. Since the 2D profile is constant, α_0 is independent of θ , same for α since there are no twist.

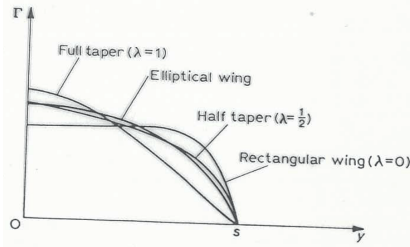


Figure 51

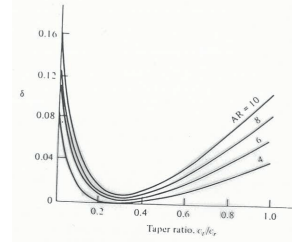


Figure 52

After some calculation one finds a circulation distribution as in Figure 51, where λ is defined such that $c_t = (1 - \lambda)c_r$. $\lambda = 0$ corresponds to a rectangular wing and $\lambda = 1$ is the triangular one. Note that the figure also represents the lift. The lift coefficient is no, because it becomes larger at the tips due to $c \searrow$. On Figure 52 is represented the induced drag coefficient δ . We see that it is always possible to find the taper ratio to have the minimum drag. Most of the planes use tapered wings since it is more simple to produce than elliptic wing.

9.5 Assume an elliptic distribution for the circulation. Show that the platform of the wing must be an ellipse.

The elliptic circulation distribution is written:

$$\Gamma(y) = \Gamma_0 \sqrt{1 - \left(\frac{y}{b/2}\right)^2}. \quad (127)$$

where Γ_0 is the circulation in the plane of symmetry. Let's compute the velocity:

$$v(y_0) = \frac{1}{4\pi} \int_{-b/2}^{b/2} \frac{d\Gamma}{y_0 - y} = \frac{\Gamma_0}{2b} = cst \quad \Rightarrow \epsilon = \alpha_i = \frac{v(y_0)}{v_\infty} = \frac{\Gamma_0}{2bv_\infty} = cst. \quad (128)$$

where we used the transformation $y = b/2 \cos \theta$. Induced angle of attack is constant along the span.

$$L'(y) = \rho v_\infty \sqrt{1 - \left(\frac{y}{b/2}\right)^2}. \quad (129)$$

On the other hand we can use (100) to express the lift as:

$$L'(y) = m(\alpha - \alpha_i - \alpha_0) \frac{1}{2} \rho_\infty v_\infty^2 c \quad (130)$$

Combining the equations we get:

$$(\alpha - \alpha_i - \alpha_0)c = \frac{2\Gamma_0}{v_\infty} \sqrt{1 - \left(\frac{y}{b/2}\right)^2}. \quad (131)$$

Note that if the left hand side is constant, the equation is satisfied for an **elliptic platform**. Since α_i is already constant, the whole term is constant only if the geometric angle of attack is constant and the profile does not change along the span. Since $C_{d_i} = C_L \alpha_i$, we can make the same analysis for the drag.

On the other hand, if the platform is non elliptic, since m varies little, the different angles must vary too. This is done by introducing a **twist** in the wing so that α varies. The lift coefficient is obtained by integration of the local lift:

$$\frac{1}{\frac{1}{2}\rho v_\infty^2 S} \int_{-b/2}^{b/2} L'(y) dy = \frac{\Gamma_0 \pi b}{2v_\infty S} = \frac{\Gamma_0 \pi}{2b v_\infty} AR. \quad (132)$$

Combination of this and what we found for α_i in this section we get:

$$\alpha_i = \frac{C_L}{\pi AR} \quad (133)$$

which is what we defined at the beginning of the chapter but for $e = 1$ (span efficiency factor). The induced drag is given by:

$$D'_i(y) = L'(y)\alpha_i \quad \Rightarrow C_{D_i} = C_L \alpha_i = \frac{C_L^2}{\pi AR}. \quad (134)$$

10 2D airfoil in compressible flow

10.1 Derive the compressible potential equation

TODO

- 10.2 Assume a thin airfoil at small angle of attack: derive the linearized potential equation. What is the range of validity as a function of the free stream Mach number**

TODO

- 10.3 Discuss the type of this equation as a function of free stream Mach number, what are the consequences**

TODO

11 2D airfoil compressible flow around an airfoil using the small perturbation approach

11.1 Derive the equation governing compressible potential equation, what are the assumptions

Remind that we have defined a potential function to describe incompressible flows, conservation of mass giving:

$$\vec{v} = \nabla \phi \quad \frac{\partial u}{\partial x} + \frac{\partial v}{\partial y} = 0 = \frac{\partial^2 \phi}{\partial x^2} + \frac{\partial^2 \phi}{\partial y^2}. \quad (135)$$

This can also be used to describe compressible flows, conservation of mass is then:

$$\rho(\phi_{xx} + \phi_{yy}) + \rho_x \phi_x + \rho_y \phi_y = 0 \quad (136)$$

where we introduced the shorthand notation $\frac{\partial a}{\partial x} = a_x$. We assume that the flow is isentropic, this is satisfied by inviscid flows (no shock wave):

$$\frac{\rho}{T^{\frac{1}{\gamma-1}}} = cst \quad \Rightarrow \frac{d\rho}{\rho} = \frac{1}{\gamma-1} \frac{dT}{T} \quad (137)$$

if the flow does not work (turbine), the temperature is constant and the equation becomes:

$$d\rho = -\frac{\rho}{2a^2} d(u^2 + v^2). \quad (138)$$

If we replace the velocities we get:

$$\rho_x = -\frac{\rho}{a^2}(\phi_x \phi_{xx} + \phi_y \phi_{xy}) \quad \rho_y = -\frac{\rho}{a^2}(\phi_x \phi_{xy} + \phi_y \phi_{yy}). \quad (139)$$

That we can substitute in (136):

$$\left(1 - \frac{1}{a^2} \phi_x^2\right) \phi_{xx} + \left(1 - \frac{1}{a^2} \phi_y^2\right) \phi_{yy} - \frac{2}{a^2} \phi_x \phi_y \phi_{xy} = 0. \quad (140)$$

11.2 Derive the equation in the case of small perturbations. What are the assumptions for this equation to be valid ?

If the far field velocity profile is $u = V_\infty$, we can note the velocity field by means of perturbations: $u = V_\infty + \hat{u}$, $v = \hat{v}$. A perturbation potential function can be defined:

$$\phi = V_\infty x + \hat{\phi} \quad \text{with} \quad \hat{\phi}_x = \hat{u}, \quad \hat{\phi}_y = \hat{v}. \quad (141)$$

By substitution of this in (140):

$$\left[a^2 - (V_\infty + \hat{\phi}_x)^2\right] \hat{\phi}_{xx} + \left[a^2 - \hat{\phi}_y^2\right] \hat{\phi}_{yy} - 2(V_\infty + \hat{\phi}_x) \hat{\phi}_y \hat{\phi}_{xy} = 0. \quad (142)$$

Since the total temperature is constant:

$$\frac{a_\infty^2}{\gamma - 1} + \frac{V_\infty^2}{2} = \frac{a^2}{\gamma - 1} + \frac{(V_\infty + \hat{u})^2}{2} = \frac{\hat{v}^2}{2} \quad (143)$$

If we make the assumption of small perturbation, the quadratic terms cancel and (142) and (143) become:

$$\begin{aligned} \frac{a_\infty^2}{a^2} &= 1 - (\gamma - 1) \frac{\hat{u}}{V_\infty} M_\infty^2 \\ \left[a^2 - V_\infty^2 + 2V_\infty \hat{u}\right] \hat{\phi}_{xx} + a^2 \hat{\phi}_{yy} - 2V_\infty \hat{v} \hat{\phi}_{xy} &= 0 \\ \Rightarrow \left[1 - M_\infty^2 - (\gamma + 1) M_\infty \frac{\hat{u}}{V_\infty}\right] \hat{\phi}_{xx} + \left[1 - (\gamma - 1) M_\infty^2 \frac{\hat{u}}{V_\infty}\right] \hat{\phi}_{yy} - 2M_\infty^2 \frac{\hat{v}}{V_\infty} \hat{\phi}_{xy} &= 0 \end{aligned} \quad (144)$$

where the last expression is obtained by dividing by a_∞^2 and replacing. By considering again the small perturbation ($V_\infty \ll$) equation we get the:

Transonic small perturbation potential equation

$$\left[(1 - M_\infty^2) - (\gamma + 1) M_\infty^2 \frac{\hat{\phi}_x}{V_\infty}\right] \hat{\phi}_{xx} + \hat{\phi}_{yy} = 0. \quad (145)$$

We can see that the \hat{u} appears in $\hat{\phi}_{xx}$ term, this is no longer negligible for **sonic** velocities. For sub- and super-sonic flows however the equation simplifies in:

$$(1 - M_\infty^2) \hat{\phi}_{xx} + \hat{\phi}_{yy} = 0. \quad (146)$$

Note that we retrieve our incompressible equation for $M_\infty \rightarrow 0$. Be aware that this last relation is only valid for small perturbations (small bodies in practice) and sub- or super-sonic flows ($M_\infty > 1.2$, $M_\infty < 0.8$).

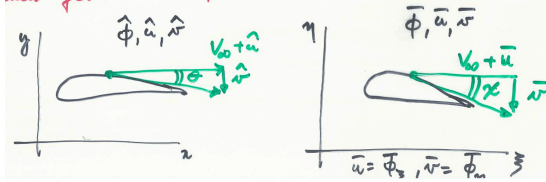
Let's now operate a change of coordinate $(x, y) \rightarrow (\xi, \eta)$, recalling $1 - M_\infty^2 \equiv \beta^2$:

$$\xi = x \quad \eta = \beta y \quad \bar{\phi}(\xi, \eta) = m \cdot \hat{\phi}(x, y) \quad (147)$$

where m is a constant. Let's find the expression of $\bar{\phi}(\xi, \eta)$. The chain rule gives:

$$\begin{aligned} \hat{\phi}_x &= \hat{\phi}_\xi = \frac{1}{m} \bar{\phi}_\xi & \hat{\phi}_y &= \frac{\beta}{m} \bar{\phi}_\eta & \hat{\phi}_{xx} &= \frac{1}{m} \bar{\phi}_{\xi\xi} & \hat{\phi}_{yy} &= \frac{\beta^2}{m} \bar{\phi}_{\eta\eta} \\ &&&&&&& \Rightarrow \bar{\phi}_{xx} + \bar{\phi}_{yy} = 0 \end{aligned} \quad (148)$$

We can see that the compressible flow in (x, y) is reduced to an incompressible flow in the (ξ, η) plane. Pay attention that $\bar{\phi}$ describes the perturbation velocities \bar{u}, \bar{v} in the (ξ, η) plane.



We can now focus on the shape of the profile in the new axis. Let's analyze the tangent to the profile by defining the angle θ for the profile in (x, y) . Under the assumption of small perturbation (thin airfoil), we can see that:

$$\tan \theta \approx \theta = \frac{\hat{v}}{V_\infty + \hat{u}} \approx \frac{\hat{v}}{V_\infty} = \frac{1}{V_\infty} \hat{\phi}_y \quad \Rightarrow \chi \approx \frac{1}{V_\infty} \bar{\phi}_\eta \quad (149)$$

where the analogy for the new plane is done. Using (148), we get:

$$\theta = \frac{\beta}{m} \chi. \quad (150)$$

Let's investigate two cases:

- If we choose $m = \beta$, $\theta = \chi$, the two profiles are identical. We have for the velocity:

$$\hat{u} = \hat{\phi}_x = \frac{\bar{\phi}_\xi}{\beta} = \frac{\bar{u}}{\beta} \quad (151)$$

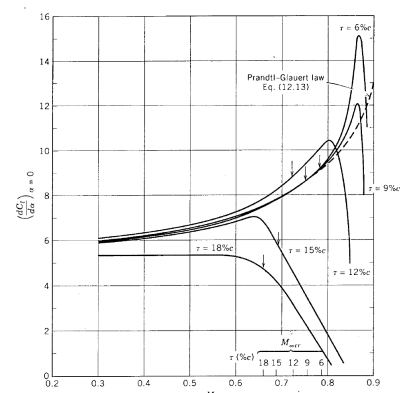
and since the pressure coefficient is given by $C_p = -\frac{2\hat{u}}{V_\infty}$:

Prandtl-Glauert rule

$$C_p = \frac{C_{p,inc}}{\beta} = \frac{C_{p,inc}}{\sqrt{1 - M_\infty^2}}. \quad (152)$$

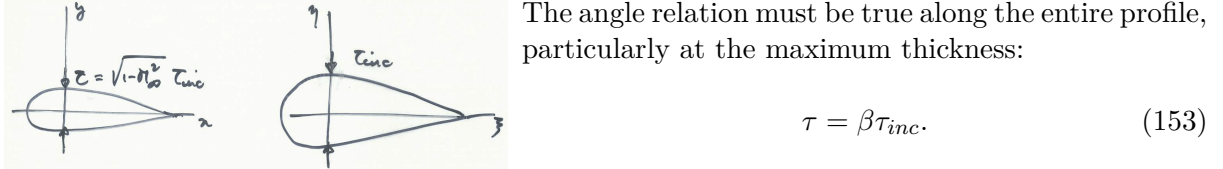
This equation allows us to compute the pressure distribution in compressible flow, beginning from the incompressible one.

Since the lift and moment coefficient are given by the integration of the pressure coefficient along the wing, we have the same result for them (so also the slope of lift curve m). Here is plotted the experimental data and the approximated m by means of the above relation for $\alpha = 0$ and for different airfoil thickness τ . We can see that for the thinner wings, we have a good agreement, until we reach the **critical Mach number** (Mach number at infinity for which Mach number 1 is reached on the profile).



This value exceeded, we have shock waves (formula valid only for Mach until 0.8). For thicker wings, we see that the slope m is always underestimated. The critical Mach number is here much lower.

- If we choose $m = 1, \hat{u} = \bar{u}$ so that $C_p = C_{p,inc}$. We see that the pressure coefficient is now the same but the profiles are different following we are in the compressible or incompressible case $\theta = \beta\chi$.



Remark 1 If we take into account the aspect ratio, we can rewrite the slope m as:
Figure 55

$$m = \frac{m_{inc}}{\beta} \frac{2\pi}{\beta \left(1 + \frac{2}{eAR}\right)} \quad (154)$$

where we used the theoretical 2D slope 2π . Another possibility is to write the lift as:

$$c_l = \frac{2\pi}{\beta} (\alpha - \alpha_{L_0} - \alpha_i) = \frac{2\pi}{\beta + \frac{2}{eAR}} (\alpha - \alpha_{L_0}) \quad (155)$$

We can last note the existence of the DATCOM formula that accounts for the effect of the aspect ratio, sweep angle Λ , Mach number and has also a correction factor for viscous effects $\kappa \approx 0.97$:

$$m = \frac{2\pi AR}{2 + \sqrt{\frac{AR^2 + \beta^2}{\kappa^2} \left(1 + \frac{\tan^2 \Lambda}{\beta^2}\right) + 4}}. \quad (156)$$

Remark 2 We can also rearrange the expression of C_p with the approximation of small angles, we had:

$$C_p = \frac{p - p_\infty}{\frac{1}{2}\rho_\infty V_\infty^2} = \frac{\gamma 2p_\infty}{\gamma \rho_\infty V_\infty^2} \left(\frac{p}{p_\infty} - 1\right) = \frac{2}{\gamma M_\infty^2} \left(\frac{p}{p_\infty} - 1\right) \quad \gamma \frac{p_\infty}{\rho_\infty} = \gamma r T = a^2 \quad (157)$$

The isentropic flow and the constant T_c give:

$$\begin{aligned} \frac{p}{p_\infty} &= \left(\frac{T}{T_\infty}\right)^{\frac{\gamma}{\gamma-1}} = \left(\frac{T_t - \frac{1}{2c_p} [(V_\infty + \hat{u})^2 + \hat{v}^2]}{T_\infty}\right)^{\frac{\gamma}{\gamma-1}} \quad T_t = T_\infty + \frac{V_\infty^2}{2c_p} \\ \Rightarrow \frac{p}{p_\infty} &= \left[1 - \frac{\gamma-1}{2} M_\infty^2 \left(\frac{2\hat{u}}{V_\infty} + \frac{\hat{u}^2 + \hat{v}^2}{V_\infty^2}\right)\right]^{\frac{\gamma}{\gamma-1}} = 1 - \frac{\gamma}{2} M_\infty^2 \left(\frac{2\hat{u}}{V_\infty} + \frac{\hat{u}^2 + \hat{v}^2}{V_\infty^2}\right) + \dots \end{aligned} \quad (158)$$

where the last expression comes from the fact that the second term is small so that we have the Taylor development of $1 + \epsilon$ (first order limited). We can neglect the second term in bracket since we have small perturbation square, and we get by (157):

$$\frac{p}{p_\infty} = -\frac{2\hat{u}}{V_\infty} \quad (159)$$

11.3 Discuss the application to an airfoil in supersonic flow: lift coefficient, influence of the Mach number, Ackeret formula, lift and drag formula

The potential equation we used in the framework of potential equation can be rewritten in the case of supersonic flow as:

$$(1 - M_\infty^2)\hat{\phi}_{xx} + \hat{\phi}_{yy} = 0 \quad \Rightarrow \lambda^2 \hat{\phi}_{xx} - \hat{\phi}_{yy} = 0. \quad (160)$$

The linearized potential equation corresponds to the wave equation with $\lambda^2 = M_\infty^2 - 1 > 0$. We can show that the solution of this equation is

$$\hat{\phi}(x, y) = f(x - \lambda y) = \hat{\phi}_1(x - \lambda y) + \hat{\phi}_2(x + \lambda y). \quad (161)$$

Let's define 2 families of characteristic curves:

$$\begin{cases} C^+ : x - \lambda y = cst & \Rightarrow y = \frac{1}{\lambda}x + cst = \frac{1}{\sqrt{M_\infty^2 - 1}}c + cst \\ C^- : x + \lambda y = cst & \Rightarrow y = -\frac{1}{\lambda}x + cst = -\frac{1}{\sqrt{M_\infty^2 - 1}}c + cst \end{cases} \quad (162)$$

In this way, $\hat{\phi}_1$ and $\hat{\phi}_2$ are respectively constant on C^+ and C^- .

The slope is denoted μ_∞^\pm for C^\pm such that:

$$\tan \mu_\infty^\pm = \pm \frac{1}{\sqrt{M_\infty^2 - 1}} \quad \sin \mu_\infty^\pm = \pm \frac{1}{M_\infty}. \quad (163)$$

To find the general solution in P, let's first consider the initial data given on the y-axis:

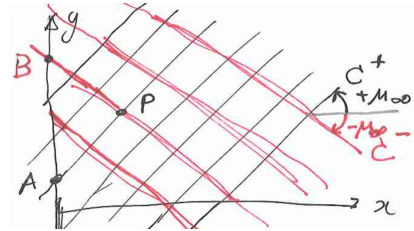


Figure 56

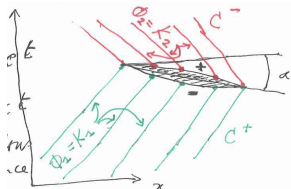
$$\hat{\phi}_1(y) = F(y) \quad \hat{\phi}_2(y) = G(y) \quad (164)$$

Now let's construct C^+ and C^- :

$$C^+ : x - \lambda y = x_A - \lambda y_A \quad C^- : x - \lambda y = x_B + \lambda y_B. \quad (165)$$

Finally, the solution in P is so given by:

$$\hat{\phi}(x_p, y_p) = \hat{\phi}(x_A - \lambda y_A) + \hat{\phi}_2(x_B + \lambda y_B) = F(x_A - \lambda y_A) + G(x_B + \lambda y_B) \quad (166)$$



Now let's define the initial conditions at $x = 0$ for small α for a thin profile:

$$F(y) = K_1 = cst \quad G(y) = K_2 = cst \quad \Rightarrow \hat{\phi} = cst \quad (167)$$

since the incoming flow is uniform. On the pressure side, we have $\hat{\phi}_1(x - \lambda y) = K_1$ which gives in the solution:

$$\hat{\phi}(q) = K_1 + \hat{\phi}_2(q) \quad \rightarrow \hat{\phi}_x = \frac{d\hat{\phi}_2}{dq} = \hat{u}^- \quad \hat{\phi}_y = \frac{d\hat{\phi}_2}{dq}\lambda = \hat{v}^- \quad \Rightarrow \hat{v}_{wall} = \lambda \hat{u}_{wall} \quad (168)$$

If we express the tangent as $\tan \theta_w \approx \theta_w = \frac{\hat{v}_w^-}{\hat{u}^- + V_\infty} \approx \frac{\hat{v}_w^-}{V_\infty}$, We can get by replacing the last results in the previous pressure coefficient equation for small perturbations:

Law of Ackeret

$$C_p^- = -\frac{2\hat{u}_w^-}{V_\infty} = -\frac{2\theta_w^-}{\sqrt{M_\infty^2 - 1}}. \quad (169)$$

The same reasoning can be done for the suction side where we'll get:

$$\hat{\phi}_x = \frac{d\hat{\phi}_1}{dq} = \hat{u}_w^+ \quad \hat{\phi}_x = \frac{d\hat{\phi}_1}{dq}(-\lambda) = \hat{v}_w^+ = -\lambda\hat{u}_w^+ \quad \Rightarrow C_p^+ = \frac{2\theta_w^+}{\sqrt{M_\infty^2 - 1}}. \quad (170)$$

11.3.1 Application to a flat plate

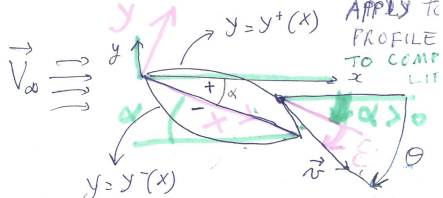


Figure 58

Consider the thin profile define by functions $y^+(x)$ and $y^-(x)$ with angles defines as:

$$\begin{aligned} \epsilon &= \frac{dy}{dx} < 0 & \theta &= \frac{\hat{v}}{\hat{u} + V_\infty} < 0 \\ \Rightarrow \theta &= \epsilon - \alpha = \frac{dy}{dx} - \alpha \end{aligned} \quad (171)$$

as $\alpha > 0$. We can then apply the last formula:

$$C_p^+ = \frac{2\theta_w^+}{\sqrt{M_\infty^2 - 1}} = \frac{2\left(\frac{dy^+}{dx} - \alpha\right)}{\sqrt{M_\infty^2 - 1}} \quad C_p^- = -\frac{2\theta_w^-}{\sqrt{M_\infty^2 - 1}} = \frac{2\left(\alpha - \frac{dy^-}{dx}\right)}{\sqrt{M_\infty^2 - 1}}. \quad (172)$$

We are now interested in computing the normal and tangential force applied on the wing, for a counter-clock contour:

$$C_N = \int_0^1 C_p^- \frac{dx}{c} + \int_1^0 C_p^+ \frac{dx}{c} = \frac{4\alpha}{\sqrt{M_\infty^2 - 1}} \quad (173)$$

where we replace the C_p 's by their definition and we neglect $\frac{dy}{dx}$ terms. For the drag we have the same procedure but by neglecting this time α :

$$\begin{aligned} C_\Gamma &= -\int_0^1 C_p^- \frac{dy}{c} - \int_1^0 C_p^+ \frac{dy}{c} = \frac{2}{\sqrt{M_\infty^2 - 1}} \left[\int_0^1 \left(\frac{dy^-}{dx} \right)^2 \frac{dx}{c} + \int_0^1 \left(\frac{dy^+}{dx} \right)^2 \frac{dx}{c} \right] \\ \Rightarrow C_\Gamma &= \frac{2}{\sqrt{M_\infty^2 - 1}} [I^- + I^+] \end{aligned} \quad (174)$$

To compute the lift and drag coefficient we only have to make the projections, and in case of flat plate $\frac{dy}{dx} = 0 = I^\pm$:

$$\begin{aligned} C_l &= -C_\Gamma \sin \alpha + C_N \cos \alpha \approx -\alpha C_\Gamma + C_N & C_d &= C_\Gamma + \alpha C_N \\ \Rightarrow C_l &= \frac{4\alpha}{\sqrt{M_\infty^2 - 1}} & C_d &= \frac{4\alpha}{\sqrt{M_\infty^2 - 1}}. \end{aligned} \quad (175)$$

The drag is the **wave drag**.

11.4 What is wave drag ? discuss supersonic flow over double wedge profile

A wave drag is a drag due to a shock wave. When a shock wave appears, it uses energy, which has to be provided by the aircraft, it is thus seen as a drag.

If we apply the Ackeret law to this profile we have:

$$\begin{aligned} C_{p1} &= \frac{2(\delta - \alpha)}{\sqrt{M_\infty^2 - 1}} & C_{p2} &= \frac{2(\delta + \alpha)}{\sqrt{M_\infty^2 - 1}} \\ C_{p3} &= \frac{-2(\delta + \alpha)}{\sqrt{M_\infty^2 - 1}} & C_{p4} &= \frac{-2(\delta - \alpha)}{\sqrt{M_\infty^2 - 1}} \end{aligned} \quad (176)$$

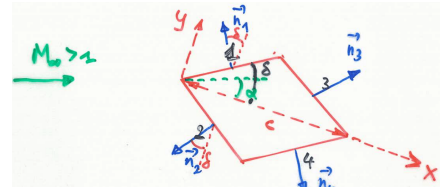


Figure 59

We can compute the lift and drag coefficients by integrating over the surface:

$$\begin{aligned} \vec{F} &= - \oint p d\vec{S} = - \oint (p - p_\infty) d\vec{S} = - \frac{1}{2} \rho_\infty V_\infty^2 \oint C_p d\vec{S} \\ \Rightarrow \vec{F}_1 &= - \frac{1}{2} \rho_\infty V_\infty^2 C_{p1} \frac{c}{2} \vec{n}_1 \end{aligned} \quad (177)$$

If we make the force non dimensional:

$$\vec{C}_1 = \frac{\vec{F}_1}{\frac{1}{2} \rho_\infty V_\infty^2 c} = - \frac{C_{p1}}{2} \vec{n}_1 \quad \Rightarrow \vec{C}_i = - \frac{C_{pi}}{2} \vec{n}_i \quad (178)$$

If we look to the normal and tangent forces we find:

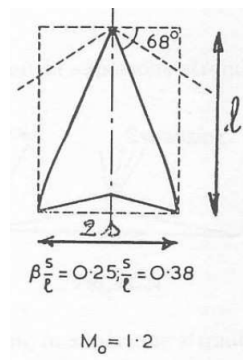
$$\begin{aligned} C_y &= \vec{C}_i \cdot \vec{i}_y = \left(-\frac{C_{p1}}{2} + \frac{C_{p2}}{2} - \frac{C_{p3}}{2} + \frac{C_{p4}}{2} \right) \cos \delta = \frac{4\alpha}{\sqrt{M_\infty^2 - 1}} \cos \delta \approx \frac{4\alpha}{\sqrt{M_\infty^2 - 1}} \\ C_x &= \vec{C}_i \cdot \vec{i}_x = \left(\frac{C_{p1}}{2} + \frac{C_{p2}}{2} - \frac{C_{p3}}{2} - \frac{C_{p4}}{2} \right) \sin \delta = \frac{4\delta}{\sqrt{M_\infty^2 - 1}} \sin \delta \approx \frac{4\delta^2}{\sqrt{M_\infty^2 - 1}} \end{aligned} \quad (179)$$

Then we make the same projection as previously:

$$c_l \approx C_y - \alpha C_x = \frac{4\alpha}{\sqrt{M_\infty^2 - 1}} - \frac{4\delta^2 \alpha}{\sqrt{M_\infty^2 - 1}} \approx \frac{4\alpha}{\sqrt{M_\infty^2 - 1}} \quad (180)$$

We find thus the same lift coefficient as the flat plate. Let's see the drag:

$$c_d = C_x + \alpha C_y = \frac{4\delta}{\sqrt{M_\infty^2 - 1}} + \frac{4\alpha}{\sqrt{M_\infty^2 - 1}}, \quad (181)$$



where the first term is **incidence wave drag** (result of lift), the same as the flat plate and the second term the **thickness wave drag** (result of volume) corresponding to the drag of the wedge at 0 degrees and angle of attack. The following empirical formula can be used for both drag on wing and on **complete plane**:

$$C_{Dw} = k_0 \frac{128}{\pi} \frac{V^2}{Sl^4} + k_1 \frac{1}{2\pi} \frac{S}{l^2} \lambda^2 C_L^2 \quad (182)$$

where k_0 and k_1 are constant of order 1 depending on the geometry and l the average length as represented on the figure.

Figure 60

11.5 Transonic flow over a profile: what is critical free stream Mach number(+ discussion), what is drag divergence Mach number

11.5.1 Critical Mach number

The critical Mach Number is the M_∞ when $M = 1$ somewhere on the airfoil. Consider a point A, the drag is given by:

$$C_{p,A} = \frac{2}{\gamma M_\infty^2} \left(\frac{p_A}{p_\infty} - 1 \right) \quad (183)$$

If we combine the fact that the flow is isentropic:

$$\frac{p_A}{p_\infty} = \left(\frac{T_A}{T_\infty} \right)^{\frac{\gamma}{\gamma-1}} = \left(\frac{1 + \frac{\gamma-1}{2} M_\infty^2}{1 + \frac{\gamma-1}{2} M_A^2} \right)^{\frac{\gamma}{\gamma-1}} \Rightarrow C_{p,A} = \frac{2}{\gamma M_\infty^2} \left[\left(\frac{1 + \frac{\gamma-1}{2} M_\infty^2}{1 + \frac{\gamma-1}{2} M_A^2} \right)^{\frac{\gamma}{\gamma-1}} - 1 \right] \quad (184)$$

If now we consider $M_\infty = M_{kr} \rightarrow M_A = 1$, so that the equation becomes:

$$C_{p,A} = \frac{2}{\gamma M_\infty^2} \left[\left(\frac{1 + \frac{\gamma-1}{2} M_\infty^2}{1 + \frac{\gamma-1}{2} M_A^2} \right)^{\frac{\gamma}{\gamma-1}} - 1 \right] \quad C_{p,A} = \frac{C_{p,A,inc}}{\sqrt{1 - M_{kr}^2}}, \quad (185)$$

where the second equation is the Prandtl-Glauert relation. We can plot the two equations on a graph. The intersection of the two graphs gives the critical Mach number. We can see that the minimum lift coefficient at low velocities is more negative than the thin case, characterized by a smaller M_{kr} . The perturbation of the flow is higher. Flying at high subsonic velocities is important \rightarrow thin airfoil. When the angle of attack increases, the lift increases but the higher velocity on the suction part makes the M_{kr} much lower. We want so the wing to be as thin as possible but we are limited by the structural strength and the fuel storage.

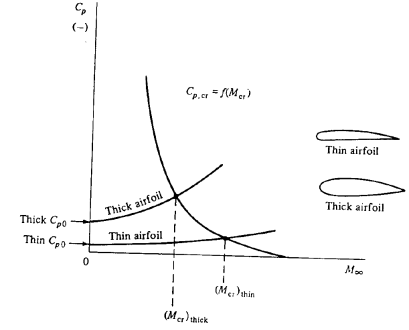


Figure 61

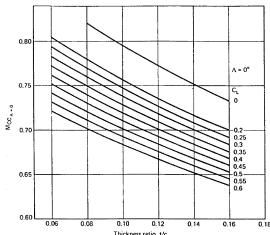


Figure 62

We avoid also large bending of the leading edge to avoid large accelerations. One solution to increase M_{kr} is to place the maximum camber downstream, about 50% of the chord because the velocities on the suction side will be lower. Placing it too downstream will create a too high opposite gradient and cause separation.

Symmetrical wings have a larger M_{kr} , however be careful with combination of sharp LE because of LE separation. In practice we have a quasi-symmetrical profile with camber near LE. Swept wings also increase the M_{kr} .

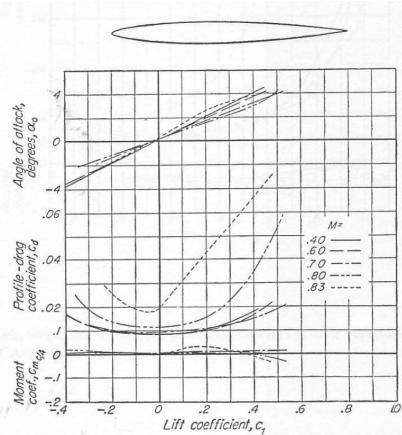


Figure 63

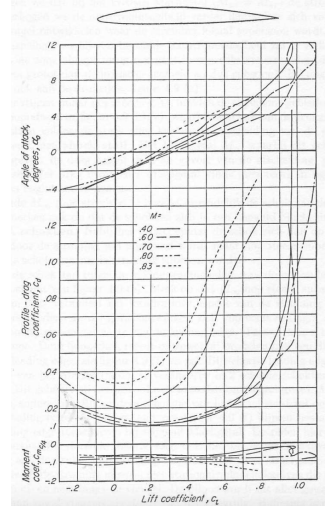


Figure 64

We can observe here above, the plot of α , C_L and C_D for a symmetrical and a non-symmetrical airfoil. We can observe on Figure 63 that the slope of the lift curve goes up to $M = 0.83$ (Prandtl-Glauert). Once above M_{kr} it starts to decrease and the drag suddenly increases.

On Figure 64 we can see similar effects at the difference that around M_{kr} we have a positive increase of the zero lift angle, having a negative effect on longitudinal stability. Note that the decrease of the lift curve starts earlier, M_{kr} is smaller.

11.5.2 Drag divergence Mach number

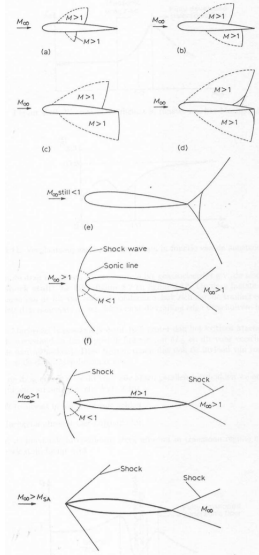


Figure 65

At the critical Mach number $M_\infty = M_{cr}$, the flow reaches $M = 1$ somewhere on the wing. If the velocity at ∞ is increased, M_∞ also (still < 0), a small area where the flow becomes **supersonic** will develop on the **suction side**. For increasing M_∞ this area will grow and at a certain M_∞ a **shock wave** will develop, as a result of which the flow will become **subsonic** again (the supersonic area abruptly terminated). Such area also develops on the **pressure side** at high M_∞ (Figure 65 (a)).

If M_∞ increases further, the supersonic regions further extends and the shock waves move downstream, the one on the pressure side more rapidly (Figure 65 (b) (c)). As soon as the shock waves are strong enough, they can cause separation of the boundary layer, this separation is the **shock stall** and the M_∞ where this happens is called the **drag divergence Mach number**. Indeed, the drag suddenly increases as a result of the separation, this called **transonic drag rise**, shown on Figure 66.

For further increase of $M_\infty < 1$, the shock wave on the pressure side eventually reaches the trailing edge (Figure 65 (d)). In a certain Mach number range, the shock wave manifests the so-called **λ shocks**. Near the profile the shock has two legs, a first oblique one through which the flow is slowed down but remains supersonic, and a second normal one

through which the flow becomes subsonic.

Eventually the shock wave on the suction side can also reach the trailing edge and give birth to the **bifurcated trailing edge shock pattern** (Figure 65 (e)).

For further increase of M_∞ there is no change, till M_∞ exceeds 1. In this case, a so-called **detached bow shock** develops upstream of the leading edge. There is a small subsonic region between this shock and the leading edge. This manifests both for thick, bounded leading edge and thin one (Figure 65 (f) (g)). In the second case, the bow shock changes into 2 oblique shocks at the leading edge for increasing M_∞ (Figure 65 (h)). This happens at the **shock attachment Mach number**, M_{SA} . For further M_∞ , the flow becomes fully supersonic and the drag decreases. In the case of rounded leading edge, the bow shock continues to exist and comes closer to the leading edge.

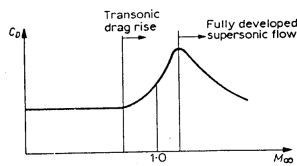


Figure 66

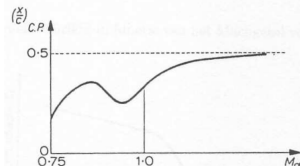


Figure 67

Under transonic conditions the flow is non-stationary, the shock waves moves up and down on the wing. The pilot senses this as **buffeting** (response of the structure to aerodynamic excitation) and vibrations. This can make the plane uncontrollable or cause serious damages. The cause of the excitation is the fluctuating pressure in non-stationary conditions. Normally one flies under the buffeting margin but one can exceed it in case of sudden maneuvers for fighters for example.

The center of pressure is also moving with M_∞ (Figure 67). First, it goes backward as the shock wave going backward on the suction side makes the underpressure greater. Then, it goes forward because the shock wave on the pressure side is moving faster. The latter reaches the trailing edge while the shock wave on the suction side still moves backward, making the center of pressure again move backward, tending to the 50% chord. This makes the control of the plane more difficult.

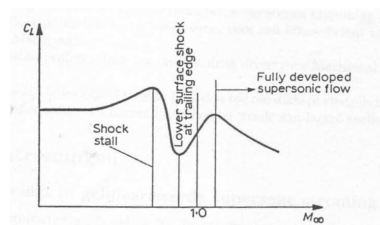


Figure 68

It is this buffeting effect that imposes an upper limit to the velocity of subsonic planes. With the increase of the drag due to separation when shock waves (shock-stall) is associated a decrease of the lift. We can see that the lift temporary increases after the lower shock reaches the trailing edge. This is explained by the smaller separation when in this location. The drag divergence Mach number is 5-10% larger than M_{cr} .

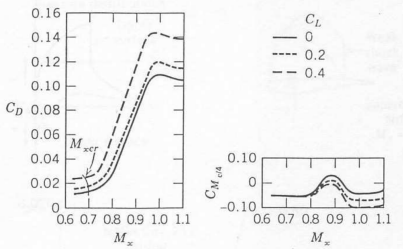


Figure 69

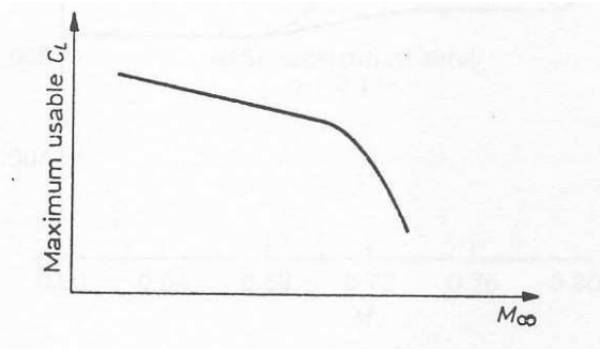


Figure 70

On Figure 69 we can see the influence of increasing lift (increasing α). We can notice that with increasing lift, the drag increases for all Mach numbers, the moment increases in the transonic region and M_{cr} decreases. On Figure 70, we notice that the lift coefficient strongly decreases in the transonic region due to buffering effects.

11.6 Compute the lift coefficient for a 2D profile in compressible flow, assuming that the lift coefficient for the same airfoil is known for incompressible flow.

Using Prandtl-Glauert : $C_p = \frac{C_{p,inc}}{\beta} = \frac{C_{p,inc}}{\sqrt{1-M_\infty^2}}$. Since lift is an integration of pressure: $C_L = \frac{C_{L,inc}}{\beta} = \frac{C_{L,inc}}{\sqrt{1-M_\infty^2}}$

11.7 Discuss the graph giving the slope of the lift curve as a function of the free stream Mach number ($M_{infinity}$)

TODO

12 Discuss effect of sweep on performance of a 3D wing in compressible flow – Influence on Lift and drag

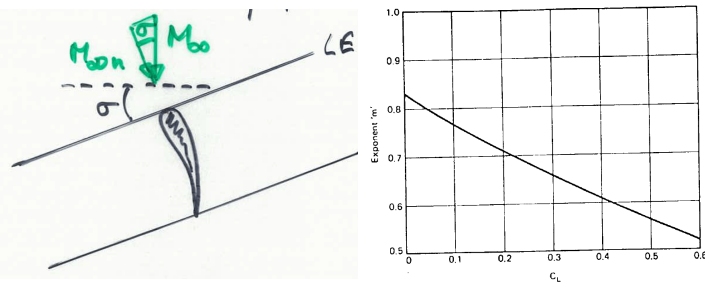


Figure 71

Figure 72

This is a technique used in order to increase the critical mach number. Indeed, the flow seen by the 2D wing is the one perpendicular to the wing:

$$V_{\infty n} = V_\infty \cos \sigma \quad \Rightarrow M_{kr}^\sigma = \frac{M_{kr}^{\sigma=0}}{\cos^m \sigma} \quad (186)$$

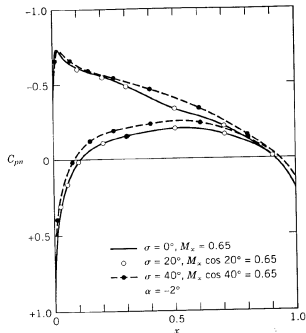
where we can see that the M_{∞} will be higher and where m varying parameter in function of the C_L , it decreases with lift (Figure 72). If the sweep angle is large enough, the flow seen by the LE can become subsonic and allow rounded shapes which is advantageous for subsonic speeds. The drag divergence mach number also increases:

$$M_{div} = M_{kr}[1.02 + 0.08(1 - \cos \sigma)]. \quad (187)$$

12.1 Lift of swept wings

Remind the definition of C_p :

$$C_{pn} = \frac{p - p_{\infty}}{\frac{1}{2}\rho_{\infty}V_{\infty}^2} \quad L_n = \frac{1}{2}\rho_{\infty}V_{\infty}^2 \int_{LE}^{TE} (C_{pln} - C_{pun}) dx \quad (188)$$



where we see that if $M_{\infty n} = M_{\infty}^*$ (M_{∞}^* in this case is the one we have without sweep), the pressure distribution and thus the lift remains constant. This means that for a same approaching speed V_{∞}^* without and with sweep we will decrease the lift (we have to fly at higher speed). The lift coefficient also decreases for $V_{\infty n} = V_{\infty}^*$:

$$c_l^* = \frac{L^*}{\frac{1}{2}\rho_{\infty}V_{\infty}^*} > c_l = \frac{L^*}{\frac{1}{2}\rho_{\infty}V_{\infty}} \quad (189)$$

where * designate the same value in non swept wing. We see that the lift coefficient decreases.

Pay attention that this is the case when we are in subsonic flight. Indeed, the sweep increases the lift for supersonic as the shock stall is postponed ($M_{\infty n}$ seen smaller). In practice, to have significant influence of sweep σ must be high (at least 30°- 40°).

12.2 Lift coefficient as a function of the angle of attack for swept wings

As we have seen, the lift and the lift coefficient decreases when sweep wings. This implies that the slope of the lift curve is also smaller. Remark that we have the same AR in the figure, in practice the AR of swept wing is smaller than the one without (2 to 4 - sweep, 6 to 10 - subsonic), but the lift slope is even smaller.

There are structural advantages as it allows to have thinner airfoils (better for high speed), and the M_{kr} increases. To increase the structural strength we use **taper** (chord decreases from root to tip). This smaller AR induces more drag, demanding more take-off and landing distance. The reduced slope of lift requires high α when landing and take-off (Concorde drooped nose), but there is no pronounced stall limit.

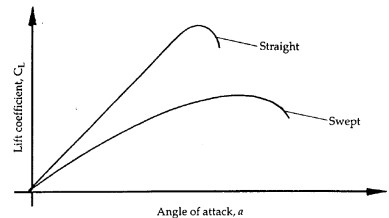


Figure 75

12.3 Influence of the sweep angle on the drag

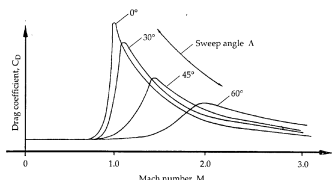


Figure 76

One observes the increase of M_{div} , the decrease of the maximum drag coefficient (must have large angles to have significant effects). At sufficiently high Mach numbers, M_n will reach the supersonic limit and produce the same

effect as seen previously. In that case, the drag with no swept wing is smaller at this stage.

13 title

13.1 title

13.2 title

13.3 title